

# Provable Online CP/PARAFAC Decomposition of a Structured Tensor via Dictionary Learning

Sirisha Rambhatla, Xingguo Li, and Jarvis Haupt \*

## Abstract

We consider the problem of factorizing a structured 3-way tensor into its constituent Canonical Polyadic (CP) factors. This decomposition, which can be viewed as a generalization of singular value decomposition (SVD) for tensors, reveals how the tensor dimensions (features) interact with each other. However, since the factors are *a priori* unknown, the corresponding optimization problems are inherently non-convex. The existing guaranteed algorithms which handle this non-convexity incur an irreducible error (bias), and only apply to cases where all factors have the same structure. To this end, we develop a provable algorithm for online structured tensor factorization, wherein one of the factors obeys some incoherence conditions, and the others are sparse. Specifically we show that, under some relatively mild conditions on initialization, rank, and sparsity, our algorithm recovers the factors *exactly* (up to scaling and permutation) at a linear rate. Complementary to our theoretical results, our synthetic and real-world data evaluations showcase superior performance compared to related techniques. Moreover, its scalability and ability to learn on-the-fly makes it suitable for real-world tasks.

## 1 Introduction

Canonical Polyadic (CP) /PARAFAC decomposition aims to express a tensor as a sum of rank-1 tensors, each of which is formed by the outer-product (denoted by “ $\circ$ ”) of constituent factors columns. Specifically, the task is to factorize a given 3-way tensor  $\underline{\mathbf{Z}} \in \mathbb{R}^{n \times J \times K}$  as

$$\underline{\mathbf{Z}} = \sum_{i=1}^m \mathbf{A}_i^* \circ \mathbf{B}_i^* \circ \mathbf{C}_i^* = [[\mathbf{A}^*, \mathbf{B}^*, \mathbf{C}^*]], \quad (1)$$

where  $\mathbf{A}_i^*$ ,  $\mathbf{B}_i^*$  and  $\mathbf{C}_i^*$  are columns of factors  $\mathbf{A}^*$ ,  $\mathbf{B}^*$ , and  $\mathbf{C}^*$ , respectively, and are *a priori* unknown. A popular choice for the factorization task shown in (1) is via the alternating least squares (ALS) algorithm; see [Kolda and Bader \(2009\)](#) and references therein. Here, one can add appropriate regularization terms (such as  $\ell_1$  loss for sparsity) to the least-square objective to steer the algorithm towards specific solutions ([Martínez-Montes et al., 2008](#); [Allen, 2012](#); [Papalexakis et al., 2013](#)). However, these approaches suffer from three major issues – a) the non-convexity of associated formulations makes it challenging to establish recovery and convergence guarantees, b) one may need to solve an implicit model selection problem (e.g., choose the *a priori* unknown tensor rank  $m$ ), and c) regularization may be computationally expensive, and may not scale well in practice.

---

\*Sirisha Rambhatla is affiliated with the Computer Science Department, University of Southern California, Los Angeles, CA, USA; Email: [sirishar@usc.edu](mailto:sirishar@usc.edu). Xingguo Li is affiliated with the Computer Science Department, Princeton University, Princeton, NJ, USA; Email: [xingguo1@cs.princeton.edu](mailto:xingguo1@cs.princeton.edu). Jarvis Haupt is affiliated with Department of Electrical and Computer Engineering, University of Minnesota, Minneapolis, MN; Email: [jdhaupt@umn.edu](mailto:jdhaupt@umn.edu). This article is a preprint.

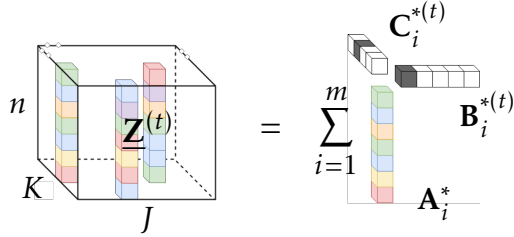


**Figure 1:** Tensor  $\underline{\mathbf{Z}}^{(t)} \in \mathbb{R}^{n \times J \times K}$  of interest, a few mode-1 fibers are dense.

Recent works for guaranteed tensor factorization – based on tensor power method (Anandkumar et al., 2015), convex relaxations (Tang and Shah, 2015), sum-of-squares formulations (Barak et al., 2015; Ma et al., 2016; Schramm and Steurer, 2017), and variants of ALS algorithm (Sharan and Valiant, 2017) – have focused on recovery of tensor factors wherein all factors have a common structure, based on some notion of incoherence of individual factor matrices such as sparsity, incoherence, or both (Sun et al., 2017). Furthermore, these algorithms a) incur *bias* in estimation, b) are computationally expensive in practice, and c) are not amenable for online (streaming) tensor factorization; See Table 1. Consequently, there is a need to develop fast, scalable provable algorithms for exact (unbiased) factorization of structured tensors arriving (or processed) in a streaming fashion (online), generated by heterogeneously structured factors. To this end, we develop a provable algorithm to recover the unknown factors of tensor(s)  $\underline{\mathbf{Z}}^{(t)}$  in Fig.1 (arriving, or made available for sequential processing, at an instance  $t$ ), assumed to be generated as (1), wherein the factor  $\mathbf{A}^*$  is *incoherent* and fixed (deterministic), and the factors  $\mathbf{B}^{*(t)}$  and  $\mathbf{C}^{*(t)}$  are sparse and vary with  $t$  (obey some randomness assumptions).

**Model Justification.** The tensor factorization task of interest arises in streaming applications where users interact only with a few items at each time  $t$ , i.e. the user-item interactions are *sparse*. Here, the fixed incoherent factor  $\mathbf{A}^*$  columns model the underlying fixed interactions patterns (*signatures*). At time  $t$ , a fresh observation tensor  $\underline{\mathbf{Z}}^{(t)}$  arrives, and the task is to estimate sparse factors (users and items), and the incoherent factor (patterns). This estimation procedure reveals users  $\mathbf{B}_i^*$  and items  $\mathbf{C}_i^*$  sharing the same pattern  $\mathbf{A}_i^*$ , i.e. the the underlying clustering, and finds applications in scrolling pattern analysis in web analytics (Mueller and Lockerd, 2001), sports analytics (section 5.2.2), patient response to probes (Deburchgraeve et al., 2009; Becker et al., 2015), electro-dermal response to audio-visual stimuli (Grundlehner et al., 2009; Silveira et al., 2013), and organizational behavior via email activity Fu et al. (2015); Kolda and Bader (2009).

## 1.1 Overview of the results

We take a matrix factorization view of the tensor factorization task to develop a provable tensor factorization algorithm for exact recovery of the constituent factors. Leveraging the structure of the tensor, we formulate the non-zero fibers as being generated by a dictionary learning model, where the data samples  $\mathbf{y}_{(j)} \in \mathbb{R}^n$  are assumed to be generated as follows from an *a priori* unknown dictionary  $\mathbf{A}^* \in \mathbb{R}^{n \times m}$  and sparse coefficients  $\mathbf{x}_{(j)}^* \in \mathbb{R}^m$ .

$$\mathbf{y}_{(j)} = \mathbf{A}^* \mathbf{x}_{(j)}^*, \quad \|\mathbf{x}_{(j)}^*\|_0 \leq s \quad \text{for all } j = 1, 2, \dots \quad (2)$$

This modeling procedure includes a matricization or *flattening* of the tensor, which leads to a Kronecker (Khatri-Rao) dependence structure among the elements of the resulting coefficient matrix;

see section 4. As a result, the main challenges here are to a) analyze the Khatri Rao product (KRP) structure to identify and quantify data samples (non-zero fibers) available for learning, b) establish guarantees on the resulting sparsity structure, and c) develop a SVD-based guaranteed algorithm to successfully untangle the sparse factors using corresponding coefficient matrix estimate and the underlying KRP structure, to develop recovery guarantees. This matricization-based analysis can be of independent interest.

## 1.2 Contributions

We develop an algorithm to recover the CP factors of tensor(s)  $\underline{\mathbf{Z}}^{(t)} \in \mathbb{R}^{n \times J \times K}$ , arriving (or made available) at time  $t$ , generated as per (1) from constituent factors  $\mathbf{A}^* \in \mathbb{R}^{n \times m}$ ,  $\mathbf{B}^{*(t)} \in \mathbb{R}^{J \times m}$ , and  $\mathbf{C}^{*(t)} \in \mathbb{R}^{K \times m}$ , where the unit-norm columns of  $\mathbf{A}^*$  obey some incoherence assumptions, and  $\mathbf{B}^{*(t)}$  and  $\mathbf{C}^{*(t)}$  are sparse. Our specific contributions are:

- **Exact recovery and linear convergence:** Our algorithm TensorNOODL, to the best of our knowledge, is the first to accomplish recovery of the true CP factors of this structured tensor(s)  $\underline{\mathbf{Z}}^{(t)}$  *exactly* (up to scaling and permutations) at a linear rate. Specifically, starting with an appropriate initialization  $\mathbf{A}^{(0)}$  of  $\mathbf{A}^*$ , we have  $\mathbf{A}_i^{(t)} \rightarrow \mathbf{A}_i^*$ ,  $\widehat{\mathbf{B}}_i^{(t)} \rightarrow \pi_{B_i} \mathbf{B}_i^{*(t)}$ , and  $\widehat{\mathbf{C}}_i^{(t)} \rightarrow \pi_{C_i} \mathbf{C}_i^{*(t)}$ , as iterations  $t \rightarrow \infty$ , for constants  $\pi_{B_i}$  and  $\pi_{C_i}$ .
- **Provable algorithm for heterogeneously-structured tensor factorization:** We consider the *exact* tensor factorization, an inherently non-convex task, when the factors do not obey same structural assumptions. That is, our algorithmic procedure overcomes the non-convexity bottleneck suffered by related optimization-based ALS formulations.
- **Online, fast, and scalable:** The online nature of our algorithm, separability of updates, and specific guidelines on choosing the parameters, make it suitable for large-scale distributed implementations. Furthermore, our numerical simulations (both synthetic and real-world) demonstrate superior performance in terms of accuracy, number of iterations, and demonstrate its applicability to real-world factorization tasks.

Furthermore, although estimating the rank of a given tensor is NP hard, the incoherence assumption on  $\mathbf{A}^*$ , and distributional assumptions on  $\mathbf{B}^{*(t)}$  and  $\mathbf{C}^{*(t)}$ , ensure that our matrix factorization view is *rank revealing* (Sidiropoulos et al., 2017). In other words, our assumptions ensure that the dictionary initialization algorithms (such as Arora et al. (2015)) can recover the rank of the tensor. Following this, TensorNOODL recovers the true factors (up to scaling and permutation) whp.

## 1.3 Related works

**Tensor Factorization.** Canonical polyadic (CP)/PARAFAC decomposition (1) captures relationships between the latent factors, where the number of rank-1 tensors define the rank for a tensor. Unlike matrices decompositions, tensor factorizations can be unique under relatively mild conditions (Kruskal, 1977; Sidiropoulos and Bro, 2000). However, determining tensor rank is NP-hard (Håstad, 1990), and so are tasks like tensor decompositions (Hillar and Lim, 2013). Nevertheless, regularized ALS-based approaches emerged as a popular choice to impose structure on the factors, however establishing convergence to even a stationary point is difficult (Mohlenkamp, 2013); see also (Cohen and Gillis, 2017). The variants of ALS with some convergence guarantees do so at the expense of complexity (Li et al., 2015; Razaviyayn et al., 2013), and convergence rate (Uchmajew, 2012); See also (Kolda and Bader, 2009) and (Sidiropoulos et al., 2017). On the other hand, guaranteed methods initially relied on a computationally expensive orthogonalizing step (*whitening*),

**Table 1:** Comparison of provable algorithms for tensor factorization and dictionary learning. As shown here, the existing provable tensor factorization techniques do not apply to the case where  $\mathbf{A}$ : incoherent,  $(\mathbf{B}, \mathbf{C})$ : sparse.

Method	Conditions			Recovery Guarantees	
	Model Considered	Rank	Initialization Constraints	Estimation Bias	Convergence
TensorNOODL (this work)	$\mathbf{A}$ : incoherent, $(\mathbf{B}, \mathbf{C})$ : sparse	$m = \mathcal{O}(n)$	$\mathcal{O}^*\left(\frac{1}{\log(n)}\right)$	No Bias	Linear
Sun et al. (2017) <sup>‡</sup>	$(\mathbf{A}, \mathbf{B}, \mathbf{C})$ : all incoherent and sparse	$m = o(n^{1.5})$	$o(1)$	$\ \mathbf{A}_{ij} - \widehat{\mathbf{A}}_{ij}\ _\infty = \mathcal{O}\left(\frac{1}{n^{0.25}}\right)^\dagger$	Not established
Sharan and Valiant (2017) <sup>‡</sup>	$(\mathbf{A}, \mathbf{B}, \mathbf{C})$ : all incoherent	$m = o(n^{0.25})$	Random	$\ \mathbf{A}_i - \widehat{\mathbf{A}}_i\ _2 = \mathcal{O}\left(\sqrt{\frac{m}{n}}\right)^\dagger$	Quadratic
Anandkumar et al. (2015) <sup>‡</sup>	$(\mathbf{A}, \mathbf{B}, \mathbf{C})$ : all incoherent	$m = \mathcal{O}(n)$	$\mathcal{O}^*\left(\frac{1}{\sqrt{n}}\right)^\P$	$\ \mathbf{A}_i - \widehat{\mathbf{A}}_i\ _2 = \widetilde{\mathcal{O}}\left(\frac{1}{\sqrt{n}}\right)^\dagger$	Linear <sup>§</sup>
		$m = o(n^{1.5})$	$\mathcal{O}(1)$	$\ \mathbf{A}_i - \widehat{\mathbf{A}}_i\ _2 = \widetilde{\mathcal{O}}\left(\sqrt{\frac{m}{n}}\right)^\dagger$	Linear
Arora et al. (2015)	Dictionary Learning (2)	$m = \mathcal{O}(n)$	$\mathcal{O}^*\left(\frac{1}{\log(n)}\right)$	$\mathcal{O}(\sqrt{s/n})$	Linear
		$m = \mathcal{O}(n)$	$\mathcal{O}^*\left(\frac{1}{\log(n)}\right)$	Negligible bias <sup>§</sup>	Linear
Mairal et al. (2009)	Dictionary Learning (2)	Convergence to stationary point; similar guarantees by Huang et al. (2016).			

<sup>‡</sup> This procedure is not *online*. <sup>†</sup> Result applies for each  $i \in [1, m]$ . <sup>‡</sup> Polynomial number of initializations  $m^{\beta^2}$  are required, for  $\beta \geq m/n$ . <sup>§</sup> The procedure has an *almost* Quadratic rate initially.

and therefore, did not extend to the overcomplete setting ( $m > n$ ) (Comon, 1994; Kolda and Mayo, 2011; Zhang and Golub, 2001; Le et al., 2011; Huang and Anandkumar, 2015; Anandkumar et al., 2014, 2016). As a result, works such as (Tang and Shah, 2015; Anandkumar et al., 2015; Sun and Luo, 2016), relaxed orthogonality to an *incoherence* condition to handle the overcomplete setting. To counter the complexity, Sharan and Valiant (2017) developed a orthogonalization-based provable ALS variant, however, this precludes its use in overcomplete settings.

**Dictionary Learning.** We now provide a brief overview of the dictionary learning literature. Popularized by the rich sparse inference literature, *overcomplete* ( $m \geq n$ ) representations lead to sparse(r) representations which are robust to noise; see Mallat and Zhang (1993); Chen et al. (1998); Donoho et al. (2006). Learning such sparsifying overcomplete representations is known as *dictionary learning* (Olshausen and Field, 1997; Lewicki and Sejnowski, 2000; Mairal et al., 2009; Gribonval and Schnass, 2010). Analogous to the ALS algorithm, the alternating minimization-based techniques became widely popular in practice, however theoretical guarantees were still limited. Provable algorithms for under- and over-complete settings were developed, however their computational complexity and initialization requirements limited their use Spielman et al. (2012); Agarwal et al. (2014); Arora et al. (2014); Barak et al. (2015). Tensor factorization algorithms have also been used to learn orthogonal (Barak et al. (2015) and Ma et al. (2016)), and convolutional (Huang and Anandkumar, 2015) dictionaries. More recently, (Rambhatla et al., 2019) proposed NOODL: a simple, scalable gradient descent-based algorithm for joint estimation of the dictionary and the coefficients, for *exact* recovery of both factors at a linear rate. Although this serves as a great starting point, tensor factorization task cannot be handled by a mere “lifting” due to the induced dependence structure.

Overall, the existing provable techniques (Table 1) in addition to being computationally expensive, incur an irreducible error (bias) in estimation and apply to cases where all factors obey the same conditions. Consequently, there is a need for fast and scalable provable tensor factorization techniques which can recover structured factors with no estimation bias.

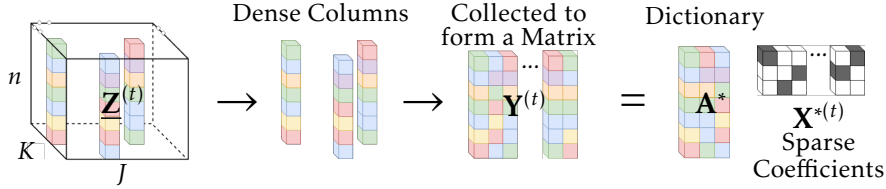


**Figure 2:** Problem Formulation: The dense columns of  $\mathbf{Z}^{(t)} \in \mathbb{R}^{n \times J \times K}$  are collected in a matrix  $\mathbf{Y}^{(t)}$ . Then  $\mathbf{Y}^{(t)}$  is viewed as arising from a dictionary learning model.

**Notation.** Bold, lower-case ( $\mathbf{v}$ ) and upper-case ( $\mathbf{M}$ ) letters, denote vectors and matrices, respectively. We use  $\mathbf{M}_i$ ,  $\mathbf{M}_{(i,:)}$ ,  $\mathbf{M}_{ij}$  (also  $\mathbf{M}(i, j)$ ), and  $\mathbf{v}_i$  (also  $\mathbf{v}(i)$ ) to denote the  $i$ -th column,  $i$ -th row,  $(i, j)$  element, respectively. We use “ $\odot$ ” and “ $\otimes$ ” to denote the Khatri-Rao (column-wise Kronecker product) and Kronecker product, respectively. Next, we use  $(\cdot)^{(n)}$  to denote the  $n$ -th iterate, and  $(\cdot)_{(n)}$  for the  $n$ -th data sample. We also use standard Landau notations  $\mathcal{O}(\cdot)$ ,  $\Omega(\cdot)$  ( $\widetilde{\mathcal{O}}(\cdot)$ ,  $\widetilde{\Omega}(\cdot)$ ) to denote the asymptotic behavior (ignoring log factors). Also, for a constant  $L$  (independent of  $n$ ), we use  $g(n) = \mathcal{O}^*(f(n))$  to indicate that  $g(n) \leq Lf(n)$ . We use  $c(\cdot)$  for constants determined by the quantities in  $(\cdot)$ . Also, we define  $\mathcal{T}_\tau(z) := z \cdot \mathbb{1}_{|z| \geq \tau}$  as the hard-thresholding operator, where “ $\mathbb{1}$ ” is the indicator function, and  $\text{supp}(\cdot)$  for the support (set of non-zero elements) and  $\text{sign}(\cdot)$  for element-wise sign. Also,  $(\cdot)^{(r)}$  denotes potential iteration dependent parameters. See Appendix A.

## 2 Problem Formulation

Our formulation is shown in Fig. 2. Here, our aim is to recover the CP factors of tensors  $\{\underline{\mathbf{Z}}^{(t)}\}_{t=0}^{T-1}$  assumed to be generated at each iteration as per (1). Without loss of generality, let the factor  $\mathbf{A}^*$  follow some incoherence assumptions, while the factors  $\mathbf{B}^{*(t)}$  and  $\mathbf{C}^{*(t)}$  be sparse. Now, the *mode-1 unfolding* or matricization  $\mathbf{Z}_1^{(t)} \in \mathbb{R}^{JK \times n}$  of  $\underline{\mathbf{Z}}^{(t)}$  is given by

$$\mathbf{Z}_1^{(t)\top} = \mathbf{A}^* (\mathbf{C}^{*(t)} \odot \mathbf{B}^{*(t)})^\top = \mathbf{A}^* \mathbf{S}^{*(t)}, \quad (3)$$

where  $\mathbf{S}^{*(t)} \in \mathbb{R}^{m \times JK}$  is  $\mathbf{S}^{*(t)} := (\mathbf{C}^{*(t)} \odot \mathbf{B}^{*(t)})^\top$ . As a result, matrix  $\mathbf{S}^{*(t)}$  has a *transposed Khatri-Rao* structure, i.e. the  $i$ -th row of  $\mathbf{S}^{*(t)}$  is given by  $(\mathbf{C}_i^{*(t)} \otimes \mathbf{B}_i^{*(t)})^\top$ . Further, since  $\mathbf{B}^{*(t)}$  and  $\mathbf{C}^{*(t)}$  are sparse, only a few  $\mathbf{S}^{*(t)}$  columns (say  $p$ ) have non-zero elements. Now, let  $\mathbf{Y}^{(t)} \in \mathbb{R}^{n \times p}$  be a matrix formed by collecting the non-zero  $\mathbf{Z}_1^{(t)\top}$  columns, we have

$$\mathbf{Y}^{(t)} = \mathbf{A}^* \mathbf{X}^{*(t)}, \quad (4)$$

where  $\mathbf{X}^{*(t)} \in \mathbb{R}^{m \times p}$  denotes the sparse matrix corresponding to the non-zero columns of  $\mathbf{S}^{*(t)}$ . Since recovering  $\mathbf{A}^*$  and  $\mathbf{X}^{*(t)}$  given  $\mathbf{Y}^{(t)}$  is a dictionary learning task (2), we can now employ a dictionary learning algorithm (such as **NOODL**) which *exactly* recovers  $\mathbf{A}^*$  (the *dictionary*) and  $\mathbf{X}^{*(t)}$  (the *sparse coefficients*) at each time step  $t$  of the (online) algorithm. The exact recovery of  $\mathbf{X}^{*(t)}$  enables recovery of  $\mathbf{B}^{*(t)}$  and  $\mathbf{C}^{*(t)}$  using our untangling procedure.

## 3 Algorithm

We begin by presenting the algorithmic details referring to relevant assumptions, we then analyze the model assumptions and the main result in section 4. TensorNOODL (Alg. 1) operates by casting the tensor decomposition problem as a dictionary learning task. Initially, Alg. 1 is given a  $(\epsilon_0, 2)$ -

---

**Algorithm 1:** TENSORNOODL: Neurally plausible alternating Optimization-based Online Dictionary Learning for Tensor decompositions.

---

**Input:** Structured tensor  $\underline{\mathbf{Z}}^{(t)} \in \mathbb{R}^{n \times J \times K}$  at each  $t$  generated as per (1). Parameters  $\eta_A, \eta_x, \tau, T, C$ , and  $R$  as per A.3, A.5, and A.6.

**Output:** Dictionary  $\mathbf{A}^{(t)}$  and the factor estimates  $\mathbf{B}^{(t)}$  and  $\mathbf{C}^{(t)}$  (corresponding to  $\underline{\mathbf{Z}}^{(t)}$ ) at  $t$ .

**Initialize:** Estimate  $\mathbf{A}^{(0)}$ , which is  $(\epsilon_0, 2)$ -near to  $\mathbf{A}^*$  for  $\epsilon_0 = \mathcal{O}^*(1/\log(n))$ ; see Def. 1.

**for**  $t = 0$  **to**  $T - 1$  **do**

**I. Estimate Sparse Matrix  $\mathbf{X}^{*(t)}$ :**

**Initialize:**  $\mathbf{X}^{(0)(t)} = \mathcal{T}_{C/2}(\mathbf{A}^{(t)\top} \mathbf{Y}^{(t)})$  See Def.3 (5)

**for**  $r = 0$  **to**  $R - 1$  **do**

$$\mathbf{X}^{(r+1)(t)} = \mathcal{T}_{\tau^{(r)}}(\mathbf{X}^{(r)(t)} - \eta_x^{(r)} \mathbf{A}^{(t)\top} (\mathbf{A}^{(t)} \mathbf{X}^{(r)} - \mathbf{Y}^{(t)})) \quad (6)$$

**end**

$\widehat{\mathbf{X}}^{(t)} := \mathbf{X}^{(R)(t)}$ .

**II. Recover Sparse Factors  $\mathbf{B}^*$  and  $\mathbf{C}^*$ :**

Form  $\widehat{\mathbf{S}}^{(t)}$  by putting back columns of  $\widehat{\mathbf{X}}^{(t)}$  at the non-zero column locations of  $\mathbf{Z}_1^{(t)\top}$ .

$$[\widehat{\mathbf{B}}^{(t)}, \widehat{\mathbf{C}}^{(t)}] = \text{UNTANGLE-KRP}(\widehat{\mathbf{S}}^{(t)})$$

**III. Update Dictionary Factor  $\mathbf{A}^{(t)}$ :**

$$\widehat{\mathbf{g}}^{(t)} = \frac{1}{p} (\mathbf{A}^{(t)} \widehat{\mathbf{X}}_{\text{indep}}^{(t)} - \mathbf{Y}^{*(t)}) \text{sign}(\widehat{\mathbf{X}}_{\text{indep}}^{(t)})^\top \quad (7)$$

$$\mathbf{A}^{(t+1)} = \mathbf{A}^{(t)} - \eta_A \widehat{\mathbf{g}}^{(t)} \quad (8)$$

$$\mathbf{A}_i^{(t+1)} = \mathbf{A}_i^{(t+1)} / \|\mathbf{A}_i^{(t+1)}\| \quad \forall i \in [m]$$

**end**

---

close (defined below) estimate  $\mathbf{A}^{(0)}$  of  $\mathbf{A}^*$  for  $\epsilon_0 = \mathcal{O}^*(1/\log(n))$ . This initialization, which can be achieved by algorithms such as Arora et al. (2015), ensures that the estimate  $\mathbf{A}^{(0)}$  is both, column-wise and in spectral norm sense, close to  $\mathbf{A}^*$ .

**Definition 1** ( $(\epsilon, \kappa)$ -closeness) *Matrix  $\mathbf{A}$  is  $(\epsilon, \kappa)$ -close to  $\mathbf{A}^*$  if  $\|\mathbf{A} - \mathbf{A}^*\| \leq \kappa \|\mathbf{A}^*\|$ , and if there is a permutation  $\pi : [m] \rightarrow [m]$  and collection of signs  $\sigma : [m] \rightarrow \{\pm 1\}$  s.t.  $\|\sigma(i) \mathbf{A}_{\pi(i)} - \mathbf{A}_i^*\| \leq \epsilon, \forall i \in [m]$ .*

Next, we sequentially provide the tensors to be factorized,  $\{\underline{\mathbf{Z}}^{(t)}\}_{t=0}^{T-1}$  (generated independently as per (1)) at each iteration  $t$ . The algorithm proceeds in the following stages.

**I. Estimate Sparse Matrix  $\mathbf{X}^{*(t)}$ :** We use  $R$  iterative hard thresholding (IHT) steps (6) – with step-size  $\eta_x^{(r)}$  and threshold  $\tau^{(r)}$  chosen according to A.6 – to arrive at an estimate  $\widehat{\mathbf{X}}^{(t)}$  (or  $\mathbf{X}^{(R)(t)}$ ). Iterations  $R$  are determined by the target tolerance ( $\delta_R$ ) of the desired coefficient estimate, i.e. we choose  $R = \Omega(\log(1/\delta_R))$ , where  $(1 - \eta_x^{(r)})^R \leq \delta_R$ .

**II. Estimate  $\mathbf{B}^*$  and  $\mathbf{C}^*$ :** As discussed in section 2, the tensor matricization leads to a Khatri-Rao dependence structure between the factors  $\mathbf{B}^{*(t)}$  and  $\mathbf{C}^{*(t)}$ . To recover these, we develop a SVD-based algorithm (Alg. 2) to estimate sparse factors ( $\mathbf{B}^{*(t)}$  and  $\mathbf{C}^{*(t)}$ ) using an element-wise  $\zeta$ -close estimate of  $\mathbf{S}^{*(t)}$ , i.e.,  $|\widehat{\mathbf{S}}_{ij}^{(t)} - \mathbf{S}_{ij}^{*(t)}| \leq \zeta$ . Here, we form the estimate  $\widehat{\mathbf{S}}^{(t)}$  of  $\mathbf{S}^{*(t)}$  by placing columns of

---

**Algorithm 2: UNTANGLE KHATRI-RAO PRODUCT (KRP): Recovering the Sparse factors**


---

**Input:** Estimate  $\widehat{\mathbf{S}}^{(t)}$  of the KRP  $\mathbf{S}^{*(t)}$   
**Output:** Estimates  $\widehat{\mathbf{B}}^{(t)}$  and  $\widehat{\mathbf{C}}^{(t)}$  of  $\mathbf{B}^{*(t)}$  and  $\mathbf{C}^{*(t)}$ .  
**for**  $i = 1 \dots m$  **do**  
    **Reshape:**  $i$ -th row of  $\widehat{\mathbf{S}}^{(t)}$  into  $\mathbf{M}^{(i)} \in \mathbb{R}^{J \times K}$ .  
    **Set:**  $\widehat{\mathbf{B}}_i^{(t)} \leftarrow \sqrt{\sigma_1} \mathbf{u}_1$ , and  $\widehat{\mathbf{C}}_i^{(t)} \leftarrow \sqrt{\sigma_1} \mathbf{v}_1$ , where  $\sigma_1$ ,  $\mathbf{u}_1$ , and  $\mathbf{v}_1$  are the principal left and right singular vectors of  $\mathbf{M}^{(i)}$ , respectively.  
**end**

---

$\widehat{\mathbf{X}}^{(t)}$  at their corresponding locations of  $\mathbf{Z}_1^{(t)\top}$  to the Khatri-Rao structure (TensorNOODL is agnostic to the tensor structure of the data since it only operates on the non-zero fibers  $\mathbf{Y}^{(t)}$  of  $\mathbf{Z}_1^{(t)\top}$  see (4) and Fig. 2). Our recovery result for  $\widehat{\mathbf{X}}^{(t)}$  guarantees that  $\widehat{\mathbf{S}}^{(t)}$  has the same sign and support as  $\widehat{\mathbf{S}}^{*(t)}$ , we therefore provably recover the original Khatri-Rao product structure.

**III. Update  $\mathbf{A}^*$  estimate :** We use  $\mathbf{X}^{*(t)}$  estimate to update  $\mathbf{A}^{(t)}$  by an approximate gradient descent strategy (8) with step size  $\eta_A$  (A.5). The algorithm requires  $T = \max(\Omega(\log(1/\epsilon_T)), \Omega(\log(\sqrt{s}/\delta_T)))$  for  $\|\mathbf{A}_i^{(T)} - \mathbf{A}_i^*\| \leq \epsilon_T, \forall i \in [m]$  and  $|\widehat{\mathbf{X}}_{ij}^{(T)} - \mathbf{X}_{ij}^{*(t)}| \leq \delta_T$ .

**Runtime:** The runtime of TensorNOODL is  $\mathcal{O}(mnp \log(\frac{1}{\delta_r}) \max(\log(\frac{1}{\epsilon_T}), \log(\frac{\sqrt{s}}{\delta_T})))$  for  $p = \Omega(ms^2)$ . Furthermore, since  $\mathbf{X}^*$  columns can be estimated independently in parallel, TensorNOODL is scalable and can be implemented in highly distributed settings.

## 4 Main Result

We now formalize our model assumptions and state our main result; details in Appendix B.

**Model Assumptions:** First, we require that  $\mathbf{A}^*$  is  $\mu$ -incoherent (defined below), which defines the notion of incoherence for  $\mathbf{A}^*$  columns(referred to as *dictionary*).

**Definition 2** A matrix  $\mathbf{A} \in \mathbb{R}^{n \times m}$  with unit-norm columns is  $\mu$ -incoherent if for all  $i \neq j$  the inner-product between the columns of the matrix follow  $|\langle \mathbf{A}_i, \mathbf{A}_j \rangle| \leq \mu/\sqrt{n}$ .

This ensures that dictionary columns are distinguishable, akin to relaxing the orthogonality constraint. Next, we assume that sparse factors  $\mathbf{B}^{*(t)}$  and  $\mathbf{C}^{*(t)}$  are drawn from distribution classes  $\Gamma_{\alpha, C}^{\text{SG}}$  and  $\Gamma_{\beta}^{\text{Rad}}$ , respectively, here  $\Gamma_{\gamma, C}^{\text{SG}}$  and  $\Gamma_{\gamma}^{\text{Rad}}$  are defined as follows.

**Definition 3 (Distribution Class  $\Gamma_{\gamma, C}^{\text{SG}}$  and  $\Gamma_{\gamma}^{\text{Rad}}$ )** A matrix  $\mathbf{M}$  belongs to class

- $\Gamma_{\gamma}^{\text{Rad}}$ : if each entry of  $\mathbf{M}$  is independently non-zero with probability  $\gamma$ , and the values at the non-zero locations are drawn from the Rademacher distribution.
- $\Gamma_{\gamma, C}^{\text{SG}}$ : if each entry of  $\mathbf{M}$  is independently non-zero with probability  $\gamma$ , and the values at the non-zero locations are sub-Gaussian, zero-mean with unit variance and bounded away from  $C$  for some positive constant  $C \leq 1$ , i.e.,  $|\mathbf{M}_{ij}| \geq C$  for  $(i, j) \in \text{supp}(\mathbf{M})$ .

In essence, we assume that elements of  $\mathbf{B}^{*(t)}$  ( $\mathbf{C}^{*(t)}$ ) are non-zero with probability  $\alpha$  ( $\beta$ ), and that for  $\mathbf{B}^{*(t)}$  the values at the non-zero locations are drawn from a zero-mean unit-variance sub-

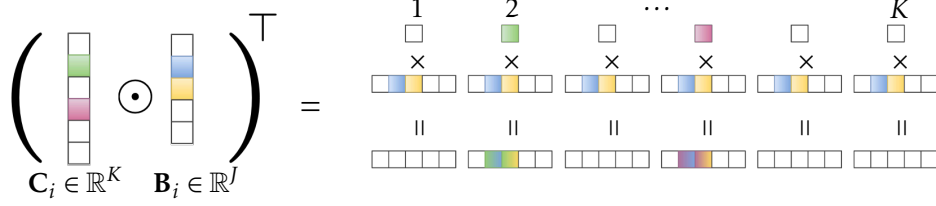


Figure 3: Transposed Khatri-Rao dependence.

Gaussian distribution, bounded away from zero, and the non-zero values of  $\mathbf{C}^{*(t)}$  are drawn from the Rademacher distribution <sup>1</sup>.

**Analyzing the Khatri-Rao Dependence:** We now turn our attention to the KR dependence structure of  $\mathbf{S}^{*(t)}$ . Fig. 3 shows a row of the matrix  $\mathbf{S}^{*(t)}$ , each entry of which is formed by multiplication of an element of  $\mathbf{C}_i^{*(t)}$  with each element of columns of  $\mathbf{B}_i^{*(t)}$ . Consequently, each row of the resulting matrix  $\mathbf{S}^{*(t)}$  has  $K$  blocks (of size  $J$ ), where the  $k$ -th block is controlled by  $\mathbf{C}_{k,i}^{*(t)}$ , and therefore the  $(i, j)$ -th entry of  $\mathbf{S}^{*(t)}$  can be written as

$$\mathbf{S}_{ij}^{*(t)} = \mathbf{C}^{*(t)}(\lfloor \frac{j}{J} \rfloor + 1, i) \mathbf{B}^{*(t)}(j - J \lfloor \frac{j}{J} \rfloor, i). \quad (9)$$

As a result, depending upon  $\alpha(\beta)$ ,  $\mathbf{S}^{*(t)}$  (consequently  $\mathbf{Z}_1^{(t)\top}$ ) may have all-zero (degenerate) columns. Therefore, we only use the non-zero columns  $\mathbf{Y}^{(t)}$  of  $\mathbf{Z}_1^{(t)\top}$ . Next, although elements in a column of  $\mathbf{S}^{*(t)}$  are independent, the KR structure induces a dependence structure across elements in a row when the elements depend on the same  $\mathbf{B}^{*(t)}$  or  $\mathbf{C}^{*(t)}$  element; see (9). In practice, we can use all non-zero columns of  $\mathbf{Z}_1^{(t)\top}$ , however for our probabilistic analysis, we require an independent set of samples. We form one such set by selecting the first column from the first block, second column from the second block and so on; see Fig. 3. This results in a  $L = \min(J, K)$  independent samples set for a given  $\mathbf{Z}_1^{(t)\top}$ . With this, and our assumptions on sparse factors ensure that the  $L$  independent columns of  $\mathbf{X}^{*(t)}$  ( $\mathbf{X}_{\text{indep}}^{*(t)}$ ) belong to the distribution class  $\mathcal{D}$  defined as follows.

**Definition 4 (Distribution class  $\mathcal{D}$ )** *The coefficient vector  $\mathbf{x}^*$  belongs to an unknown distribution  $\mathcal{D}$ , where the support  $S = \text{supp}(\mathbf{x}^*)$  is at most of size  $s$ ,  $\Pr[i \in S] = \Theta(s/m)$  and  $\Pr[i, j \in S] = \Theta(s^2/m^2)$ . Moreover, the distribution is normalized such that  $\mathbf{E}[\mathbf{x}_i^* | i \in S] = 0$  and  $\mathbf{E}[\mathbf{x}_i^{*2} | i \in S] = 1$ , and when  $i \in S$ ,  $|\mathbf{x}_i^*| \geq C$  for some constant  $C \leq 1$ . In addition, the non-zero entries are sub-Gaussian and pairwise independent conditioned on the support.*

Further, the  $(\epsilon_0, 2)$ -closeness (Def. 1) ensures that the signed-support (defined below) of the coefficients are recovered correctly (with high probability).

**Definition 5** *The signed-support of a vector  $\mathbf{x}$  is defined as  $\text{sign}(\mathbf{x}) \cdot \text{supp}(\mathbf{x})$ .*

<sup>1</sup>The non-zero entries of  $\mathbf{C}^{*(t)}$  can also be assumed to be drawn from a sub-Gaussian distribution (like  $\mathbf{B}^{*(t)}$ ) at the expense of sparsity, incoherence, dimension(s), and sample complexity. Specifically when non-zero entries of  $\mathbf{B}^{*(t)}$  and  $\mathbf{C}^{*(t)}$  are drawn from sub-Gaussian distribution (as per  $\Gamma_{\gamma, C}^{\text{SG}}$ ), we will need the dictionary learning algorithm to work with the coefficient matrix  $\mathbf{X}^{*(t)}$  (formed by product of entries of  $\mathbf{B}^{*(t)}$  and  $\mathbf{C}^{*(t)}$ ) which now has sub-Exponential non-zero entries.

**Scaling and Permutation Indeterminacy:** The unit-norm constraint on  $\mathbf{A}^*$  implies that the scaling (including the sign) ambiguity only exists in the recovery of  $\mathbf{B}^{*(t)}$  and  $\mathbf{C}^{*(t)}$ . To this end, we will regard our algorithm to be successful in the following sense.

**Definition 6 (Equivalence)** Factorizations  $[[\mathbf{A}, \mathbf{B}, \mathbf{C}]]$  are considered equivalent up to scaling, i.e.  $[[\mathbf{A}, \mathbf{B}, \mathbf{C}]] = [[\mathbf{A}^*, \mathbf{B}^* \mathbf{D}_{\sigma_b}, \mathbf{C}^* \mathbf{D}_{\sigma_c}]]$  where  $\sigma_b(\sigma_c)$  is a vector of scalings (including signs) corresponding to columns of the factors  $\mathbf{B}$  and  $\mathbf{C}$ , respectively.

**Dictionary Factor Update Strategy:** We use an *approximate* (we use an estimate of  $\mathbf{X}^{*(t)}$ ) gradient descent-based strategy (7) to update  $\mathbf{A}^{(t)}$  by finding a direction  $\mathbf{g}_i^{(t)}$  to ensure descent. Here, the  $(\Omega(s/m), \Omega(m/s), 0)$ -correlatedness (defined below) of the expected gradient vector is sufficient to make progress (“0” indicates no bias); see Candès et al. (2015); Chen and Wainwright (2015); Arora et al. (2015); Rambhatla et al. (2019).

**Definition 7** A vector  $\mathbf{g}_i^{(t)}$  is  $(\rho_-, \rho_+, \zeta_t)$ -correlated with a vector  $\mathbf{z}^*$  if for any vector  $\mathbf{z}^{(t)}$

$$\langle \mathbf{g}_i^{(t)}, \mathbf{z}^{(t)} - \mathbf{z}^* \rangle \geq \rho_- \|\mathbf{z}^{(t)} - \mathbf{z}^*\|^2 + \rho_+ \|\mathbf{g}_i^{(t)}\|^2 - \zeta_t.$$

Our model assumptions can be formalized as follows, with which we state our main result.

- A.1  $\mathbf{A}^*$  is  $\mu$ -incoherent (Def. 2), where  $\mu = \mathcal{O}(\log(n))$ ,  $\|\mathbf{A}^*\| = \mathcal{O}(\sqrt{m/n})$  and  $m = \mathcal{O}(n)$ ;
- A.2  $\mathbf{A}^{(0)}$  is  $(\epsilon_0, 2)$ -close to  $\mathbf{A}^*$  as per Def. 1, and  $\epsilon_0 = \mathcal{O}^*(1/\log(n))$ ;
- A.3 Factors  $\mathbf{B}^{*(t)}$  and  $\mathbf{C}^{*(t)}$  are respectively drawn from distributions  $\Gamma_{\alpha, C}^{\text{sG}}$  and  $\Gamma_{\beta}^{\text{Rad}}$  (Def.3);
- A.4 Sparsity controlling parameters  $\alpha$  and  $\beta$  obey  $\alpha\beta = \mathcal{O}(\sqrt{n}/m\mu \log(n))$  for  $m = \Omega(\log(\min(J, K))/\alpha\beta)$ , resulting column sparsity  $s$  of  $\mathbf{S}^{*(t)}$  is  $s = \mathcal{O}(\alpha\beta m)$ ;
- A.5 The dictionary update step-size satisfies  $\eta_A = \Theta(m/s)$ ;
- A.6 The coefficient update step-size and threshold satisfy  $\eta_x^{(r)} < c_1(\epsilon_t, \mu, n, s) = \widetilde{\Omega}(s/\sqrt{n}) < 1$  and  $\tau^{(r)} = c_2(\epsilon_t, \mu, s, n) = \widetilde{\Omega}(s^2/n)$  for small constants  $c_1$  and  $c_2$ .

**Theorem 1 (Main Result)** Suppose a tensor  $\underline{\mathbf{Z}}^{(t)} \in \mathbb{R}^{n \times J \times K}$  provided to Alg. 1 at each iteration  $t$  admits a decomposition of the form (1) with factors  $\mathbf{A}^* \in \mathbb{R}^{n \times m}$ ,  $\mathbf{B}^{*(t)} \in \mathbb{R}^{J \times m}$  and  $\mathbf{C}^{*(t)} \in \mathbb{R}^{K \times m}$  and  $\min(J, K) = \Omega(ms^2)$ . Further, suppose that the assumptions A.1-A.6 hold. Then, given  $R = \Omega(\log(n))$ , with probability at least  $(1 - \delta_{\text{alg}})$  for some small constant  $\delta_{\text{alg}}$ , the estimate  $\widehat{\mathbf{X}}^{(t)}$  at  $t$ -th iteration has the correct signed-support and satisfies

$$(\widehat{\mathbf{X}}_{i,j}^{(t)} - \mathbf{X}_{i,j}^{*(t)})^2 \leq \zeta^2 := \mathcal{O}(s(1 - \omega)^{t/2} \|\mathbf{A}_i^{(0)} - \mathbf{A}_i^*\|), \forall (i, j) \in \text{supp}(\mathbf{X}^{*(t)}).$$

Furthermore, for some  $0 < \omega < 1/2$ , the estimate  $\mathbf{A}^{(t)}$  at  $t$ -th iteration satisfies

$$\|\mathbf{A}_i^{(t)} - \mathbf{A}_i^*\|^2 \leq (1 - \omega)^t \|\mathbf{A}_i^{(0)} - \mathbf{A}_i^*\|^2, \forall t = 1, 2, \dots$$

Consequently, Alg. 2 recovers the supports of the sparse factors  $\mathbf{B}^{*(t)}$  and  $\mathbf{C}^{*(t)}$  correctly, and  $\|\widehat{\mathbf{B}}_i^{(t)} - \mathbf{B}_i^{*(t)}\|_2 \leq \epsilon_B$  and  $\|\widehat{\mathbf{C}}_i^{(t)} - \mathbf{C}_i^{*(t)}\|_2 \leq \epsilon_C$ , where  $\epsilon_B = \epsilon_C = \mathcal{O}(\frac{\zeta^2}{\alpha\beta})$ .

**Discussion:** Theorem 1 states the sufficient conditions under which, for an appropriate dictionary factor initialization (A.2), if the incoherent factor  $\mathbf{A}^*$  columns are sufficiently spread out ensuring identifiability (A.1), the sparse factors  $\mathbf{B}^{*(t)}$  and  $\mathbf{C}^{*(t)}$  are appropriately sparse (A.3 and A.4), and

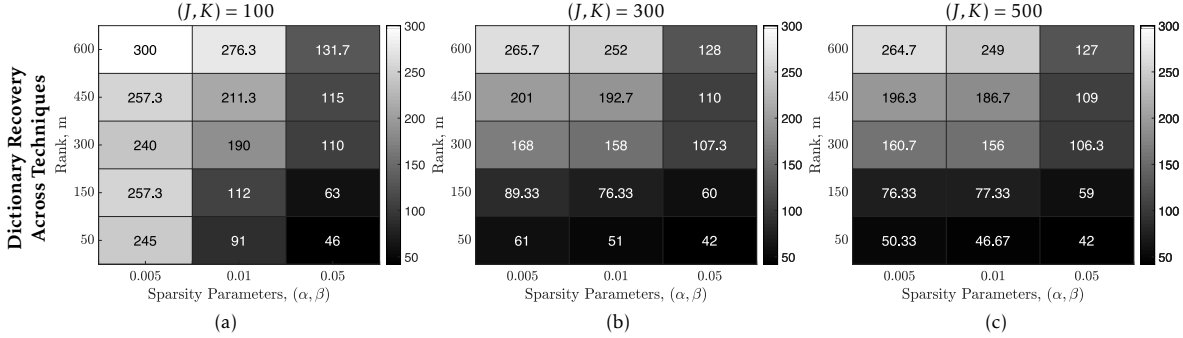


**Figure 4:** Number of iterations for convergence as a surrogate for data samples requirement <sup>2</sup>. Panels (a), (b), and (c) show the iterations taken by TensorNOODL to achieve a tolerance of  $10^{-10}$  for  $\mathbf{A}$  for  $J=K = \{100, 300, 500\}$ , respectively across ranks  $m = \{50, 150, 300, 450, 600\}$  and  $\alpha = \beta = \{0.005, 0.01, 0.05\}$ , avg. across 3 Monte Carlo runs.

for appropriately chosen learning parameters (step sizes and threshold [A.5~A.6](#)), then Alg. 1 succeeds whp. Such initializations can be achieved by existing algorithms and can also be used for model selection, i.e., determining  $m$  i.e. *revealing rank*; see [Arora et al. \(2015\)](#). Also, from [A.4](#), we observe that the sparsity  $s$  (number of non-zeros) in a column of  $\mathbf{S}^{*(t)}$  are critical for the success of the algorithm. Specifically, the upper-bound on  $s$  keeps  $s$  small for the success of dictionary learning, while the lower-bound on  $m$  for given sparsity controlling probabilities  $(\alpha, \beta)$  ensures that there are enough *independent* non-zero columns in  $\mathbf{S}^{*(t)}$  for learning. In other words, this condition ensures that sparsity is neither too low (to avoid degeneracy) nor too high (for dictionary learning), requiring that the independent samples  $L = \min(J, K) = \Omega(ms^2)$ , wherein  $s = \mathcal{O}(\alpha\beta m)$  whp.

## 5 Numerical Simulations

We evaluate TensorNOODL on synthetic and real-world data; more results in [Appendix E](#).

### 5.1 Synthetic data evaluation

**Experimental set-up:** We compare TensorNOODL with online dictionary learning algorithms presented in [Arora et al. \(2015\)](#) (Arora(b) (incurs bias) and Arora(u) (claim no bias)), and [Mairal et al. \(2009\)](#), which can be viewed as a variant of ALS (matricized) <sup>3</sup>. We analyze the recovery performance of the algorithms across different choices of tensor dimensions  $J = K = \{100, 300, 500\}$  for a fixed  $n = 300$ , rank  $m = \{50, 150, 300, 450, 600\}$ , and the sparsity parameters  $\alpha = \beta = \{0.005, 0.01, 0.05\}$  of factors  $\mathbf{B}^{*(t)}$  and  $\mathbf{C}^{*(t)}$ , across 3 Monte-Carlo runs <sup>4</sup>. We draw entries of  $\mathbf{A}^* \in \mathbb{R}^{n \times m}$  from  $\mathcal{N}(0, 1)$ , and normalize its columns to be unit-norm. To form  $\mathbf{A}^{(0)}$ , we perturb  $\mathbf{A}^*$  with random Gaussian noise and normalized its columns, such that it is column-wise  $2/\log(n)$  away from  $\mathbf{A}^*$  ([A.2](#)). To form  $\mathbf{B}^{*(t)}$  (and  $\mathbf{C}^{*(t)}$ ), we independently pick the non-zero locations with probability  $\alpha$  (and  $\beta$ ), and draw the values on the support from the Rademacher distribution <sup>5</sup>; see [Appendix E.1](#) for details.

<sup>3</sup>As discussed, the provable tensor factorization algorithms shown in [Table 1](#), are suitable only for cases wherein all the factors obey same structural assumptions, and also are not online.

<sup>3</sup> Our algorithm takes a fresh tensor at each  $t$ , we use  $T$  as a surrogate for sample requirement.

<sup>4</sup>We fix  $(J, K)$  &  $(\alpha, \beta)$ , but TensorNOODL can also be used with iteration-dependent parameters.

<sup>5</sup>The corresponding code is available at <https://github.com/srambhatla/TensorNOODL>.

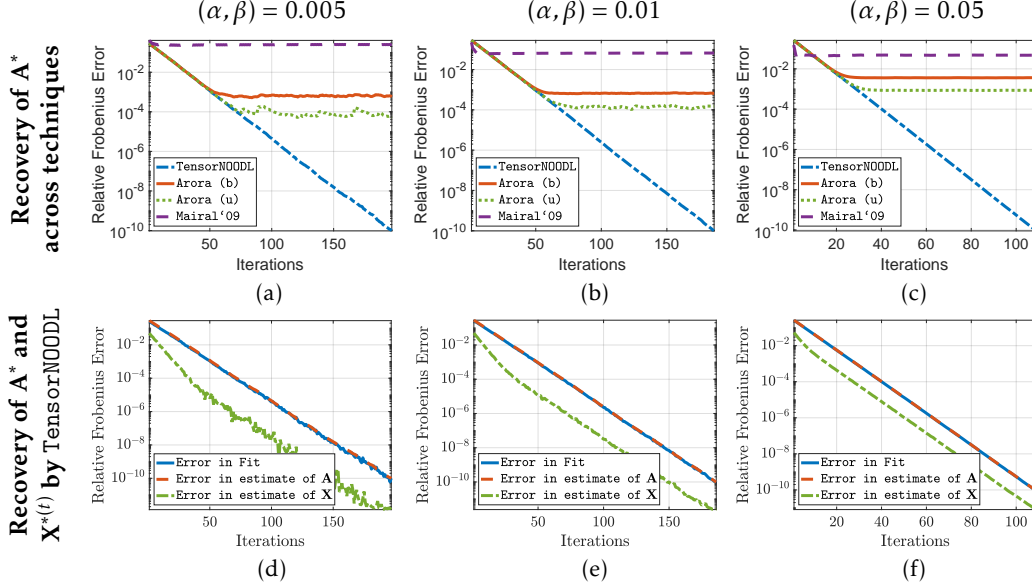


**Figure 5:** Linear convergence of TensorNOODL. Panels (a), (b), and (c) show the convergence properties of TensorNOODL, Arora (b), Arora (u) and Mairal’09 for the incoherent factor  $\mathbf{A}$  recovery for  $(\alpha, \beta) = 0.005, 0.01$  and  $0.05$  respectively for  $m = 450$ ,  $(J, K) = 500$  and  $\text{seed} = 26$ . Panels (d), (e) and (f), show the recovery of  $\mathbf{X}^{*(t)}$  (i.e.  $\mathbf{B}^{*(t)}$  and  $\mathbf{C}^{*(t)}$ )  $\mathbf{A}^*$ , and the data fit (i.e.,  $\|\mathbf{Y}^{(t)} - \mathbf{A}^{(t)}\widehat{\mathbf{X}}^{(t)}\|_{\text{F}}/\|\mathbf{Y}^{(t)}\|_{\text{F}}$ ) for TensorNOODL corresponding to (a), (b), and (c), respectively.

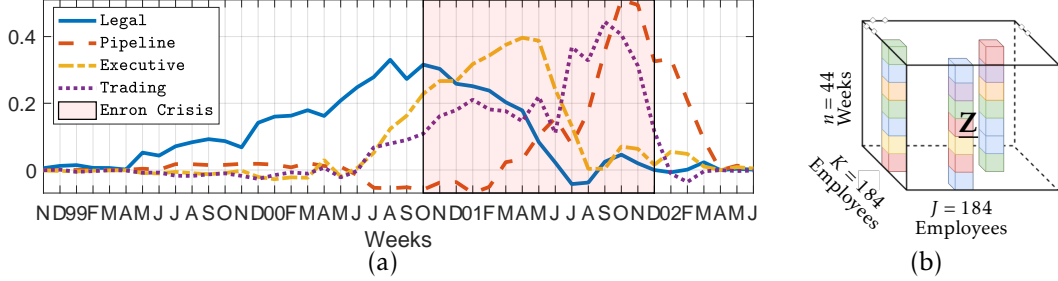
**Discussion:** We focus on the recovery of  $\mathbf{X}^{*(t)}$  (including support recovery) since the performance of Alg. 2 solely depends on exact recovery of  $\mathbf{X}^{*(t)}$ . In Fig. 4, we analyze the samples requirement across different choices of the dimension  $(J, K)$ , rank  $(m)$  and sparsity parameters  $(\alpha, \beta)$  averaged across Monte Carlo runs using the total iterations  $T^3$ . In line with theory, we observe a) in each panel the total iterations (to achieve tolerance  $\epsilon_T$ ) decreases with increasing  $(\alpha, \beta)$ , and b) for a fixed rank and sparsity parameters the  $T$  decreases with increasing  $(J, K)$ , these are both due to the increase in available data samples; also sample requirement increases with rank  $m$ . Furthermore, only TensorNOODL recovers the correct support of  $\mathbf{X}^{*(t)}$ , crucial for sparse factor recovery. Corroborating our theoretical results, TensorNOODL achieves orders of magnitude superior recovery at linear rate (Fig. 5) as compared to competing techniques both for the recovery of  $\mathbf{A}^*$ , and  $\mathbf{X}^{*(t)}$ . Moreover, since  $\mathbf{X}^*$  columns can be estimated independently, TensorNOODL is scalable and can be implemented in highly distributed settings.

## 5.2 Real-world data evaluation

We consider a real data application in sports analytics. Additional real-data experiments for an email activity-based organizational behavior application are presented in Appendix E.2.1.

### 5.2.1 Enron Email Dataset

Sparsity-regularized ALS-based tensor factorization techniques, albeit possessing limited convergence guarantees, have been a popular choice to analyze the Enron Email Dataset ( $184 \times 184 \times 44$ ) Fu et al. (2015); Bader et al. (2006). We now use TensorNOODL to analyze the email activity of 184 Enron employees over 44 weeks (Nov. ’98 –Jan. ’02) during the period before and after the financial irregularities were uncovered.



(c) Cluster Quality: False Positives/ Cluster Size

Method	Legal	Pipeline	Executive	Trading
TensorNOODL	2/13	4/11	1/14	10/24
Mairal '09	1/10	Not Found	8/17	3/7
Fu et al. (2015)	4/16	3/15	3/30 <sup>†</sup>	5/12

**Figure 6:** Enron Email Analysis. The plot and the table show the recovered group email activity patterns over time, and the cluster quality analysis, respectively. Note the increased legal team activity before the crisis broke out internally (Oct. '00), to public (Oct '01), till lay-offs. <sup>†</sup>The authors set the number of cluster to 5, here we combine the two clusters corresponding to “Executive”.

**Methodology:** For TensorNOODL and Mairal '09, we use the initialization algorithm of Arora et al. (2015), which yielded 4 dictionary elements. Following this, we use these techniques in batch setting to simultaneously identify email activity patterns and cluster employees. We also compare our results to Fu et al. (2015), which just aims to cluster the employees by imposing sparsity constraint on one of the factors, and does not learn the patterns. As opposed to Fu et al. (2015), TensorNOODL did not require us to guess the number of dictionary elements to be used. We use Alg. 2 to identify the employees corresponding to email activity patterns from the recovered sparse factors.

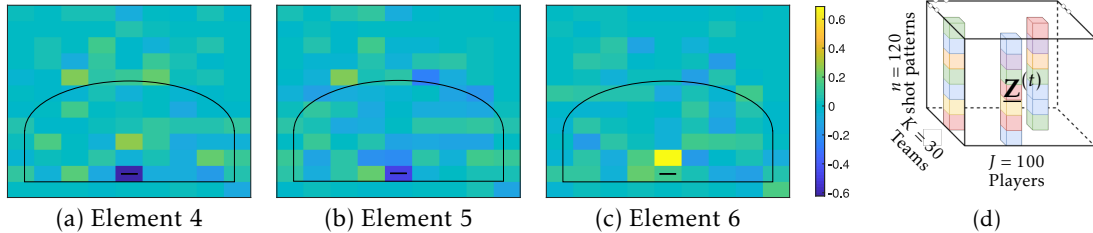
**Discussion** – Fig. 6 shows the 4 main groups of employees recovered, and their activity over time. In line with Diesner and Carley (2005), we observe that during the crisis the employees of different divisions indeed exhibited cliquish behavior. Furthermore, TensorNOODL is also superior in terms of cluster purity as inferred from the False Positives to Cluster-size ratio (Fig. 6); see Appendix E.2.1 for details.

## 5.2.2 NBA Shot Pattern Dataset

We analyze weekly shot patterns of the 100 high scoring players (80<sup>th</sup> percentile) against 30 teams in the 2018 – 19 regular season (27 weeks) of the National Basketball Association (NBA) league. The task is to identify specific shot patterns attempted by players against teams and cluster them from the weekly  $100 \times 30 \times 120$  shot pattern tensor.

**Methodology:** We divide half-court into  $10 \times 12$  blocks and sum-up all shots attempted by a player in a game from a particular block, and vectorize to form a shot pattern vector ( $\mathbb{R}^{120}$ ) of a player against a particular opponent team. We use 2017 – 18’s regular season data to initialize incoherent factor using Arora et al. (2015), recovering 7 elements.

**Discussion:** In Fig. 7 we show 3 recovered shot patterns and corresponding weights (week-10). TensorNOODL reveals the similarity in shot selection of James Harden and Devin Booker, in line with the sports reports at the time (Rafferty, 2018; Uggetti, 2018). The shared elements show their



Corresponding Sparse factor (Players) Coefficients			
Player	Element 4	Element 5	Element 6
James Harden	0.1992	0.0678	0.2834
Devin Booker	0.0114	0.0104	0.4668

**Figure 7:** NBA Regular Season Shot Pattern data analysis. TensorNOODL clusters the players and the teams. We show the three recovered dictionary factor elements (panels (a)-(c)) shared by James Harden and Devin Booker (believed to have similar styles) during week 10 of the regular season (2018 – 19). Panel (d) shows the weekly shot pattern tensor, the input for TensorNOODL at each iteration  $t$ .

shot preference above the 3-point line (Fig. 7(a-b)) and at the rim (Fig. 7(c)); See Appendix E.2.2 for detailed results, and Appendix E.2.1 for evaluations on Enron data.

## 6 Discussion

**Summary:** Leveraging a matrix view of the tensor factorization task, we propose TensorNOODL, to the best of our knowledge, the first provable algorithm to achieve exact (up to scaling and permutations) *online* structured 3-way tensor factorization at a linear rate. Our analysis to untangle the Kronecker product dependence structure (induced by the matricized view) can be leveraged by other tensor factorization tasks.

**Limitations and Future Work:** We use probabilistic model assumptions which requires us to carefully identify independent samples. Although not an issue in practice, this leads to somewhat conservative results. Future work includes improving this sample efficiency.

**Conclusions:** We analyze an exciting modality where the tensor decomposition task can be reduced to that of matrix factorization. Such correspondences offer a way to establish strong convergence and recovery guarantees for structured tensor factorization tasks.

## Acknowledgement

The authors graciously acknowledge the support from the DARPA YFA, Grant N66001-14-1-4047. The authors would also like to thank Prof. Nikos Sidiropoulos and Di Xiao for helpful discussions.

## References

AGARWAL, A., ANANDKUMAR, A., JAIN, P., NETRAPALLI, P. and TANDON, R. (2014). Learning sparsely used overcomplete dictionaries. In *COLT*.

ALLEN, G. (2012). Sparse higher-order principal components analysis. In *Artificial Intelligence and Statistics*.

- ANANDKUMAR, A., GE, R., HSU, D., KAKADE, S. M. and TELGARSKY, M. (2014). Tensor decompositions for learning latent variable models. *Journal of Machine Learning Research*, **15** 2773–2832.
- ANANDKUMAR, A., GE, R. and JANZAMIN, M. (2015). Learning overcomplete latent variable models through tensor methods. In *Conference on Learning Theory*.
- ANANDKUMAR, A., JAIN, P., SHI, Y. and NIRANJAN, U. N. (2016). Tensor vs. matrix methods: Robust tensor decomposition under block sparse perturbations. In *Artificial Intelligence and Statistics*.
- ARORA, S., GE, R., MA, T. and MOITRA, A. (2015). Simple, efficient, and neural algorithms for sparse coding. In *COLT*.
- ARORA, S., GE, R. and MOITRA, A. (2014). New algorithms for learning incoherent and overcomplete dictionaries. In *COLT*.
- BADER, B. W., HARSHMAN, R. A. and KOLDA, T. G. (2006). Pattern analysis of directed graphs using dedicom: an application to enron email. Tech. rep., Sandia National Laboratories.
- BARAK, B., KELNER, J. A. and STEURER, D. (2015). Dictionary learning and tensor decomposition via the sum-of-squares method. In *Proceedings of the forty-seventh annual ACM symposium on Theory of computing*. ACM.
- BECK, A. and TEOULLE, M. (2009). A fast iterative shrinkage-thresholding algorithm for linear inverse problems. *SIAM journal on imaging sciences*, **2** 183–202.
- BECKER, H., ALBERA, L., COMON, P., GRIBONVAL, R., WENDLING, F. and MERLET, I. (2015). Brain-source imaging: From sparse to tensor models. *IEEE Signal Processing Magazine*, **32** 100–112.
- CANDÈS, E. J., LI, X. and SOLTANOLKOTABI, M. (2015). Phase retrieval via wirtinger flow: Theory and algorithms. *IEEE Transactions on Information Theory*, **61** 1985–2007.
- CHAMBOLLE, A., VORE, R. A. D., LEE, N. Y. and LUCIER, B. J. (1998). Nonlinear wavelet image processing: variational problems, compression, and noise removal through wavelet shrinkage. *IEEE Transactions on Image Processing*, **7** 319–335.
- CHEN, S. S., DONOHO, D. L. and SAUNDERS, M. A. (1998). Atomic decomposition by basis pursuit. *SIAM Journal on Scientific Computing*, **20** 33–61.  
<https://doi.org/10.1137/S1064827596304010>
- CHEN, Y. and WAINWRIGHT, M. J. (2015). Fast low-rank estimation by projected gradient descent: General statistical and algorithmic guarantees. *CoRR*, **abs/1509.03025**.
- COHEN, J. E. and GILLIS, N. (2017). Dictionary-based tensor canonical polyadic decomposition. *IEEE Transactions on Signal Processing*, **66** 1876–1889.
- COMON, P. (1994). Independent component analysis, a new concept? *Signal processing*, **36** 287–314.
- DAUBECHIES, I., DEFRISE, M. and MOL, C. D. (2004). An iterative thresholding algorithm for linear inverse problems with a sparsity constraint. *Communications on Pure and Applied Mathematics: A Journal Issued by the Courant Institute of Mathematical Sciences*, **57** 1413–1457.

- DEBURCHGRAEVE, W., CHERIAN, P. J., VOS, M. D., SWARTE, R. M., BLOK, J. H., VISSER, G. H., GOVAERT, P. and HUFFEL, S. V. (2009). Neonatal seizure localization using parafac decomposition. *Clinical Neurophysiology*, **120** 1787–1796.
- DIESNER, J. and CARLEY, K. M. (2005). Exploration of communication networks from the enron email corpus. In *SIAM International Conference on Data Mining: Workshop on Link Analysis, Counterterrorism and Security, Newport Beach, CA*. Citeseer.
- DONOHO, D., ELAD, M. and TEMLYAKOV, V. N. (2006). Stable recovery of sparse overcomplete representations in the presence of noise. *IEEE Transactions on Information Theory*, **52** 6–18.
- FU, X., HUANG, K., MA, W. K., SIDIROPOULOS, N. D. and BRO, R. (2015). Joint tensor factorization and outlying slab suppression with applications. *IEEE Transactions on Signal Processing*, **63** 6315–6328.
- GRIBONVAL, R. and SCHNASS, K. (2010). Dictionary identification and sparse matrix-factorization via  $\ell_1$ -minimization. *IEEE Transactions on Information Theory*, **56** 3523–3539.
- GRUNDLEHNER, B., BROWN, L., PENDERS, J. and GYSELINCKX, B. (2009). The design and analysis of a real-time, continuous arousal monitor. In *2009 Sixth International Workshop on Wearable and Implantable Body Sensor Networks*. IEEE.
- HILLAR, C. J. and LIM, L. H. (2013). Most tensor problems are np-hard. *Journal of the ACM (JACM)*, **60** 45.
- HÅSTAD, J. (1990). Tensor rank is np-complete. *Journal of Algorithms*, **11** 644 – 654.  
<http://www.sciencedirect.com/science/article/pii/0196677490900146>
- HUANG, F. and ANANDKUMAR, A. (2015). Convolutional dictionary learning through tensor factorization. In *Feature Extraction: Modern Questions and Challenges*.
- HUANG, K., SIDIROPOULOS, N. D. and LIAVAS, A. P. (2016). A flexible and efficient algorithmic framework for constrained matrix and tensor factorization. *IEEE Transactions on Signal Processing*, **64** 5052–5065.
- KOLDA, T. G. and BADER, B. W. (2009). Tensor decompositions and applications. *SIAM review*, **51** 455–500.
- KOLDA, T. G. and MAYO, J. R. (2011). Shifted power method for computing tensor eigenpairs. *SIAM Journal on Matrix Analysis and Applications*, **32** 1095–1124.
- KRUSKAL, J. B. (1977). Three-way arrays: rank and uniqueness of trilinear decompositions, with application to arithmetic complexity and statistics. *Linear algebra and its applications*, **18** 95–138.
- LE, Q. V., KARPENKO, A., NGIAM, J. and NG, A. Y. (2011). Ica with reconstruction cost for efficient overcomplete feature learning. In *Advances in Neural Information Processing Systems*.
- LEWICKI, M. S. and SEJNOWSKI, T. J. (2000). Learning overcomplete representations. *Neural Comput.*, **12** 337–365.  
<http://dx.doi.org/10.1162/089976600300015826>

- LI, Z., USCHMAJEW, A. and ZHANG, S. (2015). On convergence of the maximum block improvement method. *SIAM Journal on Optimization*, **25** 210–233.
- MA, T., SHI, J. and STEURER, D. (2016). Polynomial-time tensor decompositions with sum-of-squares. In *57th Annual Symposium on Foundations of Computer Science (FOCS)*. IEEE.
- MAIRAL, J., BACH, F., PONCE, J. and SAPIRO, G. (2009). Online dictionary learning for sparse coding. In *Proceedings of the 26th Annual International Conference on Machine Learning*. ACM.
- MALLAT, S. G. and ZHANG, Z. (1993). Matching pursuits with time-frequency dictionaries. *IEEE Transactions on Signal Processing*, **41** 3397–3415.
- MARTÍNEZ-MONTES, S. E., SÁNCHEZ-BORNOT, J. M. and VALDÉS-SOSA, P. A. (2008). Penalized parafac analysis of spontaneous eeg recordings. *Statistica Sinica* 1449–1464.
- McDIARMID, C. (1998). Concentration. In *Probabilistic methods for algorithmic discrete mathematics*. Springer, 195–248.
- MOHLENKAMP, M. J. (2013). Musings on multilinear fitting. *Linear Algebra and its Applications*, **438** 834 – 852. SsTensors and Multilinear Algebra.
- MUELLER, F. and LOCKERD, A. (2001). Cheese: tracking mouse movement activity on websites, a tool for user modeling. In *CHI'01 extended abstracts on Human factors in computing systems*. ACM.
- OLSHAUSEN, B. A. and FIELD, D. J. (1997). Sparse coding with an overcomplete basis set: A strategy employed by v1? *Vision research*, **37** 3311–3325.
- PAPALEXAKIS, E. E., SIDIROPOULOS, N. D. and BRO, R. (2013). From k-means to higher-way clustering: Multilinear decomposition with sparse latent factors. *IEEE transactions on signal processing*, **61** 493–506.
- RAFFERTY, S. (2018). Devin booker has taken a page out of James Harden’s playbook – and it’s working.  
<https://ca.nba.com/news/devin-booker-assists-james-harden-comparison-huge-development-phoenix-suns/rr5zo0v7p9x41kmeyl94rmy2o>
- RAMBHATLA, S., LI, X. and HAUPT, J. (2019). NOODL: Provable online dictionary learning and sparse coding. In *International Conference on Learning Representations (ICLR)*.  
<https://openreview.net/forum?id=HJeu43ActQ>
- RAZAVIYAYN, M., HONG, M. and LUO, Z. Q. (2013). A unified convergence analysis of block successive minimization methods for nonsmooth optimization. *SIAM Journal on Optimization*, **23** 1126–1153.
- SCHRAMM, T. and STEURER, D. (2017). Fast and robust tensor decomposition with applications to dictionary learning. In *Conference on Learning Theory*.
- SHARAN, V. and VALIANT, G. (2017). Orthogonalized als: A theoretically principled tensor decomposition algorithm for practical use. In *Proceedings of the 34th International Conference on Machine Learning - Volume 70*. ICML'17, JMLR.org.  
<http://dl.acm.org/citation.cfm?id=3305890.3306001>

- SIDIROPOULOS, N. D. and BRO, R. (2000). On the uniqueness of multilinear decomposition of n-way arrays. *Journal of Chemometrics: A Journal of the Chemometrics Society*, **14** 229–239.
- SIDIROPOULOS, N. D., DE LATHAUWER, L., FU, X., HUANG, K., PAPALEXAKIS, E. E. and FALOUTSOS, C. (2017). Tensor decomposition for signal processing and machine learning. *IEEE Transactions on Signal Processing*, **65** 3551–3582.
- SILVEIRA, F., ERIKSSON, B., SHETH, A. and SHEPPARD, A. (2013). Predicting audience responses to movie content from electro-dermal activity signals. In *ACM international joint conference on Pervasive and ubiquitous computing*. ACM.
- SPIELMAN, D. A., WANG, H. and WRIGHT, J. (2012). Exact recovery of sparsely-used dictionaries. In *Conference on Learning Theory*.
- SUN, R. and LUO, Z. Q. (2016). Guaranteed matrix completion via non-convex factorization. *IEEE Transactions on Information Theory*, **62** 6535–6579.
- SUN, W. W., LU, J., LIU, H. and CHENG, G. (2017). Provable sparse tensor decomposition. *Journal of the Royal Statistical Society: Series B (Statistical Methodology)*, **79** 899–916.
- TANG, G. and SHAH, P. (2015). Guaranteed tensor decomposition: A moment approach. In *International Conference on Machine Learning*.
- TIBSHIRANI, R. (1996). Regression shrinkage and selection via the lasso. *Journal of the Royal Statistical Society. Series B (Methodological)* 267–288.
- UGGETTI, P. (2018). Devin Booker keeps climbing the ladder. When will the suns catch up? <https://www.theringer.com/nba/2019/3/28/18284788/devin-booker-phoenix-suns-dysfunction>
- USCHMAJEW, A. (2012). Local convergence of the alternating least squares algorithm for canonical tensor approximation. *SIAM Journal on Matrix Analysis and Applications*, **33** 639–652.
- YU, Y., WANG, T. and SAMWORTH, R. J. (2014). A useful variant of the davis–kahan theorem for statisticians. *Biometrika*, **102** 315–323.
- ZHANG, T. and GOLUB, G. (2001). Rank-one approximation to high order tensors. *SIAM Journal on Matrix Analysis and Applications*, **23** 534–550.

**Table 2:** Frequently used symbols: Probabilities

**Probabilities**

Symbol	Definition	Symbol	Definition
$\gamma$	$\gamma := \alpha\beta$ , where $\alpha(\beta)$ is the probability that an element $\mathbf{B}_{ij}^{*(t)}$ ( $\mathbf{C}_{ij}^{*(t)}$ ) of $\mathbf{B}^{*(t)}$ ( $\mathbf{C}^{*(t)}$ ) is non-zero.	$\delta_{\mathbf{B}_i}^{(t)}$	$\delta_{\mathbf{B}_i}^{(t)} = \exp(-\frac{\epsilon^2 J \alpha}{2(1+\epsilon/3)})$ for any $\epsilon > 0$ .
$\delta_{\mathcal{T}}^{(t)}$	$\delta_{\mathcal{T}}^{(t)} = 2m \exp(-\frac{C^2}{\mathcal{O}(\epsilon_t^2)})$	$\delta_{\beta}^{(t)}$	$2s \exp(-\frac{1}{\mathcal{O}(\epsilon_t)})$
$\delta_s^{(t)}$	$\delta_s^{(t)} = \min(J, K) \exp(-\epsilon^2 \alpha \beta m / 2(1 + \epsilon/3))$ for any $\epsilon > 0$	$\delta_p^{(t)}$	$\delta_p^{(t)} = \exp(-\frac{\epsilon^2}{2} L(1 - (1 - \gamma)^m))$
$\delta_{\text{IHT}}^{(t)}$	$\delta_{\text{IHT}}^{(t)} = \delta_{\mathcal{T}}^{(t)} + \delta_{\beta}^{(t)}$	$\delta_{\text{NOODL}}^{(t)}$	$\delta_{\text{NOODL}}^{(t)} = \delta_{\mathcal{T}}^{(t)} + \delta_{\beta}^{(t)} + \delta_{\text{HW}} + \delta_{\mathbf{g}_i}^{(t)} + \delta_{\mathbf{g}}^{(t)}$
$q_i$	$q_i = \Pr[i \in S] = \Theta(\frac{s}{m})$	$q_{i,j}$	$q_{i,j} = \Pr[i, j \in S] = \Theta(\frac{s^2}{m^2})$
$p_i$	$p_i = \mathbf{E}[\mathbf{X}_{ij}^* \text{sign}(\mathbf{X}_{ij}^*)   \mathbf{X}_{ij}^* \neq 0]$	$\delta_{\text{HW}}^{(t)}$	$\delta_{\text{HW}}^{(t)} = \exp(-1/\mathcal{O}(\epsilon_t))$
$\delta_{\mathbf{g}_i}^{(t)}$	$\delta_{\mathbf{g}_i}^{(t)} = \exp(-\Omega(s))$	$\delta_{\mathbf{g}}^{(t)}$	$\delta_{\mathbf{g}}^{(t)} = (n + m) \exp(-\Omega(m\sqrt{\log(n)}))$

## Navigating Supplementary Material

We summarize the notation used in our work in Appendix A, including with a list of frequently used symbols and their corresponding definitions. Next, in Appendix B, we present the proof of our main result, and organize the the proofs of intermediate results in Appendix C; additional results used are listed in Appendix D for completeness. Furthermore, we show the detailed synthetic and real-world experimental results, along with how to reproduce them, in Appendix E. Corresponding code with specific recommendation on the parameter setting is available at <https://github.com/srambhatla/TensorNOODL>.

## A Summary of Notation

In addition to the notation described in the manuscript, we use  $\|\mathbf{M}\|$  and  $\|\mathbf{M}\|_F$  for the spectral and Frobenius norm, respectively, and  $\|\mathbf{v}\|$ ,  $\|\mathbf{v}\|_0$ , and  $\|\mathbf{v}\|_1$  to denote the  $\ell_2$ ,  $\ell_0$  (number of non-zero entries), and  $\ell_1$  norm, respectively. In addition, we use  $\mathbf{D}_{(\mathbf{v})}$  as a diagonal matrix with elements of a vector  $\mathbf{v}$  on the diagonal. Given a matrix  $\mathbf{M}$ , we use  $\mathbf{M}_{-i}$  to denote a resulting matrix without  $i$ -th column. Also note that, since we show that  $\|\mathbf{A}_i^{(t)} - \mathbf{A}_i^*\| \leq \epsilon_t$  contracts in every step, therefore we fix  $\epsilon_t, \epsilon_0 = \mathcal{O}^*(1/\log(n))$  in our analysis. We summarize the definitions of some frequently used symbols in our analysis in Table 2 and 3.

**Table 3:** Frequently used symbols: Notation and Parameters

Symbol	Definition	Symbol	Definition
$(\cdot)^*$	Used to represent the ground-truth matrices.	$(\cdot)^{(t)}$ , $\widehat{(\cdot)}^{(t)}$ , and $\widetilde{(\cdot)}$	Used to represent the estimates formed by the algorithm.
$(\cdot)^{(t)}$	The subscript “ $t$ ” is used to represent the estimates at $t$ -iteration of the online algorithm.	$\mathbf{X}^{(r)(t)}$	The $r$ -th IHT iterate at $t$ -th iterate of the online algorithm.
$(\cdot)^{(r)}$	The subscript “ $r$ ” is used to represent the $r$ -th IHT iterate.	$\widetilde{\mathbf{X}}^{(t)}$	The final IHT estimate at ( $r = R$ ), i.e., $\mathbf{X}^{(R)(t)}$ at the $t$ -th iterate of the online algorithm.
$\mathbf{A}_i^{(t)}$	$i$ -th column of $\mathbf{A}^{(t)}$ (estimate of $\mathbf{A}^*$ at the $t$ -th iteration of the online algorithm).	$\widehat{\mathbf{B}}^{(t)}$ $(\widehat{\mathbf{C}}^{(t)})$	Estimate of $\mathbf{B}^{*(t)}$ ( $\mathbf{C}^{*(t)}$ ) at the $t$ -th iteration of the online algorithm.
$\mathbf{S}^{*(t)}$	Transposed Khatri-Rao structured (sparse) matrix, $\mathbf{S}^{*(t)} = (\mathbf{C}^{*(t)} \odot \mathbf{B}^{*(t)})^\top$ , its $i$ -th row is given by $\mathbf{C}_i^{*(t)} \otimes \mathbf{B}_i^{*(t)}$ .	$\mathbf{X}^{*(t)}$	Sparse matrix formed by collecting non-zero columns of $\mathbf{S}^{*(t)}$ .
$p$	Number of columns in $\mathbf{X}^{*(t)}$ , also the number of non-zero columns in $\mathbf{S}^{*(t)}$ .	$\mathbf{Z}_1^{(t)\top}$	Mode-1 unfolding of $\mathbf{Z}^{(t)}$ , $\mathbf{Z}_1^{(t)\top} = \mathbf{A}^*(\mathbf{C}^{*(t)} \odot \mathbf{B}^{*(t)})^\top$ at the $t$ -th iteration of the online algorithm.
$\epsilon_t$	Upper-bound on column-wise error at the $t$ -th iterate, $\ \mathbf{A}_i^{(t)} - \mathbf{A}_i^*\  \leq \epsilon_t = \mathcal{O}^*(\frac{1}{\log(n)})$ .	$\mu$	The incoherence between the columns of the factor $\mathbf{A}^*$ ; see Def. 2.
$\mu_t$	Incoherence between the columns of $\mathbf{A}^{(t)}$ , $\frac{\mu_t}{\sqrt{n}} = \frac{\mu}{\sqrt{n}} + 2\epsilon_t$ .	$\xi$	The element-wise upper bound on the error between $\widehat{\mathbf{S}}_{ij}^{(t)}$ and $\mathbf{S}_{ij}^{*(t)}$ , i.e., $ \mathbf{S}_{ij}^{*(t)} - \widehat{\mathbf{S}}_{ij}^{(t)}  \leq \xi$ .
$s$	The number of non-zeros in a column of $\mathbf{S}^{*(t)}$ , also referred to as the <i>sparsity</i> .	$\alpha(\beta)$	The probability that an element $\mathbf{B}_{ij}^{*(t)}$ ( $\mathbf{C}_{ij}^{*(t)}$ ) of $\mathbf{B}^{*(t)}$ ( $\mathbf{C}^{*(t)}$ ) is non-zero.
$\epsilon_B$	Upper-bound on column-wise $\ell_2$ -error in the estimate $\widehat{\mathbf{B}}^{(t)}$ at $t$ -th iteration, i.e., $\ \widehat{\mathbf{B}}_i^{(t)} - \mathbf{B}_i^{*(t)}\  \leq \epsilon_B = \mathcal{O}(\frac{\xi^2}{\alpha\beta})$ .	$\epsilon_C$	Upper-bound on column-wise $\ell_2$ -error in the estimate $\widehat{\mathbf{C}}^{(t)}$ at $t$ -th iteration, i.e., $\ \widehat{\mathbf{C}}_i^{(t)} - \mathbf{C}_i^{*(t)}\  \leq \epsilon_C = \mathcal{O}(\frac{\xi^2}{\alpha\beta})$ .
$R$	The total number of IHT steps at the $t$ -th iteration of the online algorithm.	$T$	Total number of online iterations.
$\delta_R$	Decay parameter for final IHT step at every $t$ , $\text{ceil}(\frac{\log(\frac{1}{\delta_R})}{\log(1 - \eta_x)}) \leq R$ , where $\eta_x$ is the step-size parameter for the IHT step.	$\delta_T$	Element-wise target error tolerance for final estimate (at $t = T$ ) of $\mathbf{X}^{*(T)}$ , $ \widehat{\mathbf{X}}_{ij}^{(T)} - \mathbf{X}_{ij}^{*(T)}  \leq \delta_T \forall i \in \text{supp}(\mathbf{X}^{*(T)})$ .
$C$	Lower-bound on $\mathbf{X}_{ij}^*$ , $ \mathbf{X}_{ij}^{*(t)}  \geq C$ for $(i, j) \in \text{supp}(\mathbf{X}^{*(t)})$ and $C \leq 1$	$L$	$L := \min(J, K)$

## B Proof of Theorem 1

In this section, we present the details of the analysis pertaining to our main result.

**Theorem 1 [Main Result]** Suppose a tensor  $\underline{\mathbf{Z}}^{(t)} \in \mathbb{R}^{n \times J \times K}$  provided to Algorithm 1 at each iteration  $t$  admits a decomposition of the form (1) with factors  $\mathbf{A}^* \in \mathbb{R}^{n \times m}$ ,  $\mathbf{B}^{*(t)} \in \mathbb{R}^{J \times m}$  and  $\mathbf{C}^{*(t)} \in \mathbb{R}^{K \times m}$  and  $\min(J, K) = \Omega(ms^2)$ . Further, suppose that the assumptions A.1-A.6 hold. Then, given  $R = \Omega(\log(n))$ , with probability at least  $(1 - \delta_{\text{alg}})$  for some small constant  $\delta_{\text{alg}}$ , the coefficient estimate  $\widehat{\mathbf{X}}^{(t)}$  at  $t$ -th iteration has the correct signed-support and satisfies

$$(\widehat{\mathbf{X}}_{i,j}^{(t)} - \mathbf{X}_{i,j}^{*(t)})^2 \leq \zeta^2 := \mathcal{O}(s(1 - \omega)^{t/2} \|\mathbf{A}_i^{(0)} - \mathbf{A}_i^*\|), \text{ for all } (i, j) \in \text{supp}(\mathbf{X}^{*(t)}).$$

Furthermore, for some  $0 < \omega < 1/2$ , the estimate  $\mathbf{A}^{(t)}$  at  $t$ -th iteration satisfies

$$\|\mathbf{A}_i^{(t)} - \mathbf{A}_i^*\|^2 \leq (1 - \omega)^t \|\mathbf{A}_i^{(0)} - \mathbf{A}_i^*\|^2, \text{ for all } t = 1, 2, \dots$$

Consequently, Algorithm 2 recovers the supports of the sparse factors  $\mathbf{B}^{*(t)}$  and  $\mathbf{C}^{*(t)}$  correctly, and  $\|\widehat{\mathbf{B}}_i^{(t)} - \mathbf{B}_i^{*(t)}\|_2 \leq \epsilon_B$  and  $\|\widehat{\mathbf{C}}_i^{(t)} - \mathbf{C}_i^{*(t)}\|_2 \leq \epsilon_C$ , where  $\epsilon_B = \epsilon_C = \mathcal{O}(\frac{\zeta^2}{\alpha\beta})$ .

Here,  $\delta_{\text{alg}} = \delta_s + \delta_p^{(t)} + \delta_{\mathbf{B}_i}^{(t)} + \delta_{\text{NOODL}}$ . Further,  $\delta_{\text{NOODL}}^{(t)} = \delta_{\mathcal{T}}^{(t)} + \delta_{\beta}^{(t)} + \delta_{\text{HW}} + \delta_{\mathbf{g}_i}^{(t)} + \delta_{\mathbf{g}}^{(t)}$ , where  $\delta_{\mathcal{T}}^{(t)} = 2m \exp(-C^2/\mathcal{O}^*(\epsilon_t^2))$ ,  $\delta_{\beta}^{(t)} = 2s \exp(-1/\mathcal{O}(\epsilon_t))$ ,  $\delta_{\text{HW}}^{(t)} = \exp(-1/\mathcal{O}(\epsilon_t))$ ,  $\delta_{\mathbf{g}_i}^{(t)} = \exp(-\Omega(s))$ ,  $\delta_{\mathbf{g}}^{(t)} = (n + m) \exp(-\Omega(m\sqrt{\log(n)}))$ . Furthermore,  $\delta_s^{(t)} = \min(J, K) \exp(-\epsilon^2 \alpha \beta m / 2(1 + \epsilon/3))$  for any  $\epsilon > 0$ ,  $\delta_p^{(t)} = \exp(-\frac{\epsilon^2}{2} L(1 - (1 - \gamma)^m))$ , and  $\delta_{\mathbf{B}_i}^{(t)} = \exp(-\frac{\epsilon^2 J \alpha}{2(1 + \epsilon/3)})$  for any  $\epsilon > 0$ . Also,  $\|\mathbf{A}_i^{(t)} - \mathbf{A}_i^*\| \leq \epsilon_t$ .

**Proof of Theorem 1** The proof procedure relies on analyzing three main steps of Alg. 1 – 1) estimating the  $\mathbf{X}^{*(t)}$  reliably corresponding to  $\underline{\mathbf{Z}}^{(t)}$ , 2) using  $\mathbf{X}^{(t)}$  to estimate the factors  $\mathbf{B}^*$  and  $\mathbf{C}^*$ , and 3) making progress on the estimate of  $\mathbf{A}^*$  at every iteration  $t$  of the online algorithm.

**Estimating the  $\mathbf{X}^{*(t)}$  reliably:** The sparse matrix  $\mathbf{X}^{*(t)}$  is formed by collecting the non-zero columns of  $\mathbf{S}^{*(t)} := (\mathbf{C}^{*(t)} \odot \mathbf{B}^{*(t)})^\top$  corresponding to  $\underline{\mathbf{Z}}^{(t)}$ . The sparsity pattern of  $\mathbf{X}^{*(t)}$  columns encodes the sparsity patterns of columns of  $\mathbf{B}^{*(t)}$  and  $\mathbf{C}^{*(t)}$ . As a result, recovering the support of  $\mathbf{X}^{*(t)}$  exactly is crucial to recover  $\mathbf{B}^*$  and  $\mathbf{C}^*$ . Furthermore, recovering the signed-support is also essential for making progress on the dictionary factor. We begin by characterizing the number of non-zeros ( $s$ ) in a column of  $\mathbf{S}^{*(t)}$  ( $\mathbf{X}^{*(t)}$ ). The number of non-zeros in a column of  $\mathbf{S}^{*(t)}$  are dependent on the non-zero elements of  $\mathbf{B}^*$  and  $\mathbf{C}^*$ . Since each element of  $\mathbf{B}^*$  ( $\mathbf{C}^*$ ) is non-zero with probability  $\alpha(\beta)$ , the upper-bound on the sparsity ( $s$ ) of  $\mathbf{S}^{*(t)}$  column is given by the following lemma.

**Lemma 1** If  $m = \Omega(\log(\min(J, K))/\alpha\beta)$  then with probability at least  $(1 - \delta_s^{(t)})$  the number of non-zeros  $s$ , in a column of  $\mathbf{S}^{*(t)}$  are upper-bounded as  $s = \mathcal{O}(\alpha\beta m)$ , where  $\delta_s^{(t)} = \min(J, K) \exp(-\epsilon^2 \alpha \beta m / 2(1 + \epsilon/3))$  for any  $\epsilon > 0$ .

In line with our intuition, the sparsity scales with the parameters  $\alpha$ ,  $\beta$  and  $m$ . Next, we focus on the Iterative Hard Thresholding (IHT) phase of the algorithm; Similar results were established in (Rambhatla et al., 2019, Lemma 1–4). Here, the first step includes recovering the correct signed-support (Def. 5) of  $\mathbf{X}^{*(t)}$  given an estimate  $\mathbf{A}^{(0)}$ , which is  $(\epsilon_0, 2)$ -near to  $\mathbf{A}^*$  for  $\epsilon_0 = \mathcal{O}^*(1/\log(n))$ ;

see Def. 1. To this end, we leverage the following lemma, to guarantee that the initialization step correctly recovers the signed-support with probability at least  $(1 - \delta_{\mathcal{T}}^{(t)})$ , for  $\delta_{\mathcal{T}}^{(t)} = 2m \exp(-\frac{C^2}{\mathcal{O}^*(\epsilon_t^2)})$ .

**Lemma 2 (Signed-support recovery)** *Suppose  $\mathbf{A}^{(t)}$  is  $\epsilon_t$ -close to  $\mathbf{A}^*$ . Then, if  $\mu = \mathcal{O}(\log(n))$ ,  $s = \mathcal{O}^*(\sqrt{n}/\mu \log(n))$ , and  $\epsilon_t = \mathcal{O}^*(1/\sqrt{\log(m)})$ , with probability at least  $(1 - \delta_{\mathcal{T}}^{(t)})$  for each random sample  $\mathbf{y} = \mathbf{A}^* \mathbf{x}^*$ :*

$$\text{sign}(\mathcal{I}_{C/2}(\mathbf{A}^{(t)})^\top \mathbf{y}) = \text{sign}(\mathbf{x}^*),$$

where  $\delta_{\mathcal{T}}^{(t)} = 2m \exp(-\frac{C^2}{\mathcal{O}^*(\epsilon_t^2)})$ .

Using Lemma 1 and 2 we also arrive at the condition that  $s = \mathcal{O}(\alpha \beta m) = \mathcal{O}^* \sqrt{n}/\mu \log(n)$ , formalized as A.4. We now use the following result to ensure that each step of the IHT stage preserves the correct signed-support. Lemma 3, states the conditions on the step size parameter  $\eta_x^{(r)}$ , and the threshold  $\tau^{(r)}$ , such that that the IHT-step preserves the correct signed-support with probability  $\delta_{\text{IHT}}^{(t)}$ , for  $\delta_{\text{IHT}}^{(t)} = 2m \exp(-\frac{C^2}{\mathcal{O}^*(\epsilon_t^2)}) + 2s \exp(-\frac{1}{\mathcal{O}(\epsilon_t)})$ .

**Lemma 3 (IHT update step preserves the correct signed-support)** *Suppose  $\mathbf{A}^{(t)}$  is  $\epsilon_t$ -close to  $\mathbf{A}^*$ ,  $\mu = \mathcal{O}(\log(n))$ ,  $s = \mathcal{O}^*(\sqrt{n}/\mu \log(n))$ , and  $\epsilon_t = \mathcal{O}^*(1/\log(m))$  Then, with probability at least  $(1 - \delta_{\beta}^{(t)} - \delta_{\mathcal{T}}^{(t)})$ , each iterate of the IHT-based coefficient update step shown in (6) has the correct signed-support, if for a constant  $c_1^{(r)}(\epsilon_t, \mu, s, n) = \widetilde{\Omega}(k^2/n)$ , the step size is chosen as  $\eta_x^{(r)} \leq c_1^{(r)}$ , and the threshold  $\tau^{(r)}$  is chosen as*

$$\tau^{(r)} = \eta_x^{(r)}(t_{\beta} + \frac{\mu_t}{\sqrt{n}} \|\mathbf{x}^{(r-1)} - \mathbf{x}^*\|_1) := c_2^{(r)}(\epsilon_t, \mu, s, n) = \widetilde{\Omega}(s^2/n),$$

for some constants  $c_1$  and  $c_2$ . Here,  $t_{\beta} = \mathcal{O}(\sqrt{s\epsilon_t})$ ,  $\delta_{\mathcal{T}}^{(t)} = 2m \exp(-\frac{C^2}{\mathcal{O}^*(\epsilon_t^2)})$ , and  $\delta_{\beta}^{(t)} = 2s \exp(-\frac{1}{\mathcal{O}(\epsilon_t)})$ .

Lemma 3 establishes condition on correct signed-support recovery by the IHT stage. We now leverage the following result, Lemma 4 to quantify the error incurred by  $\widehat{\mathbf{X}}^{(t)}$  at the end of the  $R$  IHT steps, i.e.,  $|\mathbf{X}_{ij}^{*(t)} - \widehat{\mathbf{X}}_{ij}^{(t)}| = |\mathbf{S}_{ij}^{*(t)} - \widehat{\mathbf{S}}_{ij}^{(t)}| \leq \xi$ .

**Lemma 4 (Upper-bound on the error in coefficient estimation)** *With probability at least  $(1 - \delta_{\beta}^{(t)} - \delta_{\mathcal{T}}^{(t)})$  the error incurred by each element  $(i_1, j_1) \in \text{supp}(\mathbf{X}^{*(t)})$  of the coefficient estimate is upper-bounded as*

$$|\widehat{\mathbf{X}}_{i_1 j_1}^{(t)} - \mathbf{X}_{i_1 j_1}^{*(t)}| \leq \mathcal{O}(t_{\beta}) + \left( (R+1)s\eta_x \frac{\mu_t}{\sqrt{n}} \max_{(i,j)} |\mathbf{X}_{ij}^{(0)(t)} - \mathbf{X}_{ij}^{*(t)}| + |\mathbf{X}_{i_1 j_1}^{(0)(t)} - \mathbf{X}_{i_1 j_1}^{*(t)}| \right) \delta_R = \mathcal{O}(t_{\beta})$$

where  $t_{\beta} = \mathcal{O}(\sqrt{s\epsilon_t})$ ,  $\delta_R := (1 - \eta_x + \eta_x \frac{\mu_t}{\sqrt{n}})^R$ ,  $\delta_{\mathcal{T}}^{(t)} = 2m \exp(-\frac{C^2}{\mathcal{O}^*(\epsilon_t^2)})$ ,  $\delta_{\beta}^{(t)} = 2s \exp(-\frac{1}{\mathcal{O}(\epsilon_t)})$ , and  $\mu_t$  is the incoherence between the columns of  $\mathbf{A}^{(t)}$ .

Also, the corresponding expression for  $\widehat{\mathbf{X}}^{(t)}$ , which facilitates the analysis of the dictionary updates, is given by Lemma 5.

**Lemma 5 (Expression for the coefficient estimate at the end of  $R$ -th IHT iteration)** *With probability at least  $(1 - \delta_{\mathcal{T}}^{(t)} - \delta_{\beta}^{(t)})$  the  $i$ -th element of the coefficient estimate, for each  $i \in \text{supp}(\mathbf{x}^*)$ , is given by*

$$\widehat{\mathbf{x}}_i := \mathbf{x}_i^{(R)} = \mathbf{x}_i^*(1 - \lambda_i^{(t)}) + \vartheta_i^{(R)}.$$

Here,  $|\vartheta_i^{(R)}| = \mathcal{O}(t_\beta)$ , where  $t_\beta = \mathcal{O}(\sqrt{s\epsilon_i})$ . Further,  $\lambda_i^{(t)} = |\langle \mathbf{A}_i^{(t)} - \mathbf{A}_i^*, \mathbf{A}_i^* \rangle| \leq \frac{\epsilon_i^2}{2}$ ,  $\delta_T^{(t)} = 2m \exp(-\frac{C^2}{\mathcal{O}^*(\epsilon_i^2)})$  and  $\delta_\beta^{(t)} = 2s \exp(-\frac{1}{\mathcal{O}(\epsilon_i)})$ .

Interestingly, Lemma 4 shows that the error in the non-zero elements of  $\widehat{\mathbf{X}}$  only depends on the error in the incoherent factor (dictionary)  $\mathbf{A}^{(t)}$ , which results in the following expression for  $\xi^2$ .

$$\xi^2 := \mathcal{O}(s(1-\omega)^{t/2} \|\mathbf{A}_i^{(0)} - \mathbf{A}_i^*\|), \text{ for all } (i, j) \in \text{supp}(\mathbf{X}^*). \quad (10)$$

Therefore, if the the column-wise error in the dictionary decreases at each iteration  $t$ , then the IHT-based sparse matrix estimates also improve progressively.

**Recover Sparse Factors  $\mathbf{B}^*$  and  $\mathbf{C}^*$  via Alg.2:** The results for the IHT-stage are foundational for the recovery of the sparse tensor factors  $\mathbf{B}^{*(t)}$  and  $\mathbf{C}^{*(t)}$  since they a) ensure correct signed-support recovery, guaranteed by Lemma 3 and b) establish an upper-bound on the estimation error in  $\widehat{\mathbf{S}}^{(t)}$ . With these results, we now establish the correctness of Alg. 2 given an entry-wise  $\zeta$ -close estimate of  $\mathbf{S}^{*(t)}$ ,  $|\widehat{\mathbf{S}}_{ij}^{(t)} - \mathbf{S}_{ij}^{*(t)}| \leq \zeta$  given by the IHT stage. This procedure recovers the sparse factors  $\mathbf{B}^{*(t)}$  and  $\mathbf{C}^{*(t)}$ , given element-wise  $\xi$ -close estimate  $\widehat{\mathbf{S}}$  of  $\mathbf{S}^{*(t)}$ . The following lemma establishes recovery guarantees on the sparse factors using the SVD-based Alg. 2, up to sign and scaling ambiguity.

**Lemma 6** Suppose the input  $\widehat{\mathbf{S}}^{(t)}$  to Alg. 2 is entry-wise  $\zeta$  close to  $\mathbf{S}^{*(t)}$ , i.e.,  $|\widehat{\mathbf{S}}_{ij}^{(t)} - \mathbf{S}_{ij}^{*(t)}| \leq \zeta$  and has the correct signed-support as  $\mathbf{S}^{*(t)}$ . Then with probability atleast  $(1 - \delta_{\text{IHT}}^{(t)} - \delta_{\mathbf{B}_i}^{(t)})$ , both  $\widehat{\mathbf{B}}_i^{(t)}$  and  $\widehat{\mathbf{C}}_i^{(t)}$  have the correct support, and  $\left\| \frac{\mathbf{B}_i^{(t)}}{\|\mathbf{B}_i^{*(t)}\|} - \pi_i \frac{\widehat{\mathbf{B}}_i^{(t)}}{\|\widehat{\mathbf{B}}_i^{(t)}\|} \right\| = \mathcal{O}(\zeta^2)$  and  $\left\| \frac{\mathbf{C}_i^{*(t)*}}{\|\mathbf{C}_i^{*(t)}\|} - \pi_i \frac{\widehat{\mathbf{C}}_i^{(t)}}{\|\widehat{\mathbf{C}}_i^{(t)}\|} \right\| = \mathcal{O}(\zeta^2)$ , where  $\delta_{\text{IHT}}^{(t)} = 2m \exp(-\frac{C^2}{\mathcal{O}^*(\epsilon_i^2)}) + 2s \exp(-\frac{1}{\mathcal{O}(\epsilon_i)})$  for  $\|\mathbf{A}_i^{(t)} - \mathbf{A}_i^*\| \leq \epsilon_t$ , and  $\delta_{\mathbf{B}_i}^{(t)} = \exp(-\frac{\epsilon^2 J \alpha}{2(1+\epsilon/3)})$  for any  $\epsilon > 0$ .

Here, we have used  $\delta_{\text{IHT}}^{(t)} = \delta_\beta^{(t)} + \delta_T^{(t)}$  for simplicity.

**Update Dictionary Factor  $\mathbf{A}^{(t)}$ :** The update of the dictionary factor involves concentration results which rely on an independent set of data samples. For this, notice that the  $i$ -th row of  $\mathbf{S}^{*(t)}$  can be written as  $(\mathbf{C}_i^{*(t)} \otimes \mathbf{B}_i^{*(t)})^\top$ . Now, since  $\mathbf{B}^{*(t)}$  and  $\mathbf{C}^{*(t)}$  are sparse, there are a number of columns in  $\mathbf{S}^{*(t)}$  which are degenerate (all-zeros). As a result, the corresponding data samples (columns of  $\mathbf{Z}_1^{(t)\top}$ ) are also degenerate, and cannot be used for learning. Furthermore, due to the dependence structure in  $\mathbf{S}^{*(t)}$  (discussed in section 4) some of the data samples are dependent on each other, and at least from the theoretical perspective, are not eligible for the learning process. Therefore, we characterize the expected number of viable data samples in the following lemma.

**Lemma 7** For  $L = \min(J, K)$ ,  $\gamma = \alpha\beta$ , and any  $\epsilon > 0$  and suppose we have

$$L \geq \frac{2}{(1-(1-\gamma)^m)\epsilon^2} \log\left(\frac{1}{\delta_p^{(t)}}\right),$$

then with probability at least  $(1 - \delta_p)$ ,

$$p = L(1 - (1 - \gamma)^m),$$

where  $\delta_p^{(t)} = \exp(-\frac{\epsilon^2}{2} L(1 - (1 - \gamma)^m))$ .

Here, we observe that the number of viable samples increase with number of independent samples  $L = \min(J, K)$ , sparsity parameter  $\gamma = \alpha\beta$ , and rank of the decomposition  $m$ . To recover the incoherent (dictionary) factor  $\mathbf{A}^*$ , we follow analysis similar to (Rambhatla et al., 2019, Lemma 5-9). Here, we first develop an expression for the expected gradient vector in Lemma 8.

**Lemma 8 (Expression for the expected gradient vector)** *Suppose that  $\mathbf{A}^{(t)}$  is  $(\epsilon_t, 2)$ -near to  $\mathbf{A}^*$ . Then, the dictionary update step in Alg. 1 amounts to the following for the  $j$ -th dictionary element*

$$\mathbf{E}[\mathbf{A}_j^{(t+1)}] = \mathbf{A}_j^{(t)} + \eta_A \mathbf{g}_j^{(t)},$$

where for a small  $\tilde{\gamma}$ ,  $\mathbf{g}_j^{(t)}$  is given by

$$\mathbf{g}_j^{(t)} = q_j p_j \left( (1 - \lambda_j^{(t)}) \mathbf{A}_j^{(t)} - \mathbf{A}_j^* + \frac{1}{q_j p_j} \Delta_j^{(t)} \pm \tilde{\gamma} \right),$$

$\lambda_j^{(t)} = \langle \mathbf{A}_j^{(t)} - \mathbf{A}_j^*, \mathbf{A}_j^* \rangle$ , and  $\Delta_j^{(t)} := \mathbf{E}[\mathbf{A}_S^{(t)} \mathfrak{S}_S^{(R)} \text{sign}(\mathbf{x}_j^*)]$ , where  $\|\Delta_j^{(t)}\| = \mathcal{O}(\sqrt{m} q_{i,j} p_j \epsilon_t \|\mathbf{A}^{(t)}\|)$ .

Since we use empirical gradient estimate, the following lemma establishes that the empirical gradient vector concentrates around its mean, and that it make progress at each step.

**Lemma 9 (Concentration of the empirical gradient vector)** *Given  $p = \tilde{\Omega}(mk^2)$  samples, the empirical gradient vector estimate corresponding to the  $i$ -th dictionary element,  $\widehat{\mathbf{g}}_i^{(t)}$  concentrates around its expectation, i.e.,*

$$\|\widehat{\mathbf{g}}_i^{(t)} - \mathbf{g}_i^{(t)}\| \leq o\left(\frac{s}{m} \epsilon_t\right).$$

with probability at least  $(1 - \delta_{\mathbf{g}_i}^{(t)} - \delta_{\beta}^{(t)} - \delta_{\mathcal{T}}^{(t)} - \delta_{\text{HW}}^{(t)})$ , where  $\delta_{\mathbf{g}_i}^{(t)} = \exp(-\Omega(s))$ .

We then leverage Lemma 10 to show that the empirical gradient vector  $\widehat{\mathbf{g}}_j^{(t)}$  is correlated with the descent direction (see Def. 7), which ensures that the dictionary estimate makes progress at each iteration of the online algorithm.

**Lemma 10 (Empirical gradient vector is correlated with the descent direction)** *Suppose  $\mathbf{A}^{(t)}$  is  $(\epsilon_t, 2)$ -near to  $\mathbf{A}^*$ ,  $s = \mathcal{O}(\sqrt{n})$  and  $\eta_A = \mathcal{O}(m/s)$ . Then, with probability at least  $(1 - \delta_{\mathcal{T}}^{(t)} - \delta_{\beta}^{(t)} - \delta_{\text{HW}}^{(t)} - \delta_{\mathbf{g}}^{(t)})$  the empirical gradient vector  $\widehat{\mathbf{g}}_j^{(t)}$  is  $(\Omega(k/m), \Omega(m/k), 0)$ -correlated with  $(\mathbf{A}_j^{(t)} - \mathbf{A}_j^*)$ , and for any  $t \in [T]$ ,*

$$\|\mathbf{A}_j^{(t+1)} - \mathbf{A}_j^*\|^2 \leq (1 - \rho_- \eta_A) \|\mathbf{A}_j^{(t)} - \mathbf{A}_j^*\|^2.$$

This step also requires closeness that the estimate  $\mathbf{A}^{(t)}$  and  $\mathbf{A}^*$  are close, both column-wise and in the spectral norm-sense, as per Def 1. To this end, we show that the updated dictionary matrix maintain the closeness property. For this, we first show that the gradient matrix concentrates around its mean in Lemma 11.

**Lemma 11 (Concentration of the empirical gradient matrix)** *With probability at least  $(1 - \delta_{\beta}^{(t)} - \delta_{\mathcal{T}}^{(t)} - \delta_{\text{HW}}^{(t)} - \delta_{\mathbf{g}}^{(t)})$ ,  $\|\widehat{\mathbf{g}}^{(t)} - \mathbf{g}^{(t)}\|$  is upper-bounded by  $\mathcal{O}^*(\frac{s}{m} \|\mathbf{A}^*\|)$ , where  $\delta_{\mathbf{g}}^{(t)} = (n + m) \exp(-\Omega(m\sqrt{\log(n)}))$ .*

Further, the closeness property is maintained, as shown below.

**Lemma 12 ( $\mathbf{A}^{(t+1)}$  maintains closeness)** *Suppose  $\mathbf{A}^{(t)}$  is  $(\epsilon_t, 2)$  near to  $\mathbf{A}^*$  with  $\epsilon_t = \mathcal{O}^*(1/\log(n))$ , and number of samples used in step  $t$  is  $p = \tilde{\Omega}(ms^2)$ , then with probability at least  $(1 - \delta_{\mathcal{T}}^{(t)} - \delta_{\beta}^{(t)} - \delta_{\text{HW}}^{(t)} - \delta_{\mathbf{g}}^{(t)})$ ,  $\mathbf{A}^{(t+1)}$  satisfies  $\|\mathbf{A}^{(t+1)} - \mathbf{A}^*\| \leq 2\|\mathbf{A}^*\|$ .*

Therefore, the recovery of factor  $\mathbf{A}^*$ , and the sparse-structured matrix  $\mathbf{X}^*$  succeeds with probability  $\delta_{\text{NOODL}}^{(t)} = \delta_T^{(t)} + \delta_\beta^{(t)} + \delta_{\text{HW}} + \delta_{\mathbf{g}_i}^{(t)} + \delta_{\mathbf{g}}^{(t)}$ , where  $\delta_T^{(t)} = 2m \exp(-C^2/\mathcal{O}^*(\epsilon_t^2))$ ,  $\delta_\beta^{(t)} = 2s \exp(-1/\mathcal{O}(\epsilon_t))$ ,  $\delta_{\text{HW}}^{(t)} = \exp(-1/\mathcal{O}(\epsilon_t))$ ,  $\delta_{\mathbf{g}_i}^{(t)} = \exp(-\Omega(s))$ ,  $\delta_{\mathbf{g}}^{(t)} = (n+m)\exp(-\Omega(m\sqrt{\log(n)}))$ .

Further, from Lemma 1, we have that the columns of  $\mathbf{S}^{*(t)}$  are  $s = \mathcal{O}(\alpha\beta m)$  sparse with probability  $(1 - \delta_s^{(t)})$ , where  $\delta_s^{(t)} = \min(J, K) \exp(-\epsilon^2 \alpha \beta m / 2(1 + \epsilon/3))$  for any  $\epsilon > 0$ , and that with probability at least  $(1 - \delta_p)$ , the number of data samples  $p = L(1 - (1 - \gamma)^m)$ , where  $\delta_p^{(t)} = \exp(-\frac{\epsilon^2}{2} L(1 - (1 - \gamma)^m))$  using Lemma 1. Furthermore, from Lemma 6, we know that Alg. 2 (which only relies on recovery of  $\mathbf{X}^{*(t)}$ ) succeeds in recovering  $\mathbf{B}^{*(t)}$  and  $\mathbf{C}^{*(t)}$  (upto permutation and scaling) with probability  $(1 - \delta_{\mathbf{B}_i}^{(t)})$ , where  $\delta_{\mathbf{B}_i}^{(t)} = \exp(-\frac{\epsilon^2 J \alpha}{2(1 + \epsilon/3)})$  for any  $\epsilon > 0$ . Combining all these results we have that, Alg. 1 succeeds with probability  $(1 - \delta_{\text{alg}})$ , where  $\delta_{\text{alg}} = \delta_s + \delta_p^{(t)} + \delta_{\mathbf{B}_i}^{(t)} + \delta_{\text{NOODL}}$ . Also, the total run time of the algorithm is  $\mathcal{O}(mnp \log(1/\delta_R) \max(\log(1/\epsilon_T), \log(\sqrt{s}/\delta_T)))$  for  $p = \Omega(ms^2)$ . Hence, our main result.

**A note on independent sample requirement:** Since the IHT-based coefficient operates independently on each column of  $\mathbf{Y}^{(t)}$  (the non-zero columns of  $\mathbf{Z}_1^{(t)\top}$ ), the dependence structure of  $\mathbf{S}^{*(t)}$  does not affect this stage. For the dictionary update (in theory) we only use the independent columns of  $\mathbf{Y}^{(t)}$ , these can be inferred using  $J$  and  $K$ , and corresponding induced transposed Khatri-Rao structure. In practice, we don't need to throw away any samples, this is purely to ensure that the independence assumption holds for our finite sample analysis of the algorithm. ■

## C Proof of Intermediate Results

**Lemma 1** *If  $m = \Omega(\log(\min(J, K))/\alpha\beta)$  then with probability at least  $(1 - \delta_s^{(t)})$  the number of non-zeros,  $s$ , in a column of  $\mathbf{S}^{*(t)}$  are upper-bounded as  $s = \mathcal{O}(\alpha\beta m)$ , where  $\delta_s^{(t)} = \min(J, K) \exp(-\epsilon^2 \alpha \beta m / 2(1 + \epsilon/3))$  for any  $\epsilon > 0$ .*

**Proof of Lemma 1** Consider a column of the transposed Khatri-Rao structured matrix  $\mathbf{S}^{*(t)}$  defined as  $\mathbf{S}^{*(t)} = (\mathbf{C}^{*(t)} \odot \mathbf{B}^{*(t)})^\top$ . Here, since the entries of factors  $\mathbf{B}^{*(t)}$  and  $\mathbf{C}^{*(t)}$  are independently non-zero with probability  $\alpha$  and  $\beta$ , respectively, each entry of a column of  $\mathbf{S}^{*(t)}$  is independently non-zero with probability  $\gamma = \alpha\beta$ , i.e.,  $\mathbb{1}_{|\mathbf{s}_{ij}^{*(t)}| > 0} \sim \text{Bernoulli}(\gamma)$ . As a result, the number of non-zero elements in a column of  $\mathbf{S}^{*(t)}$  are Binomial( $m, \gamma$ ).

Now, let  $\mathbf{s}_{ij}$  be the indicator for the  $(i, j)$  element of  $\mathbf{S}^{*(t)}$  being non-zero, defined as

$$\mathbf{s}_{ij} = \mathbb{1}_{|\mathbf{s}_{ij}^{*(t)}| > 0}.$$

Then, the expected number of non-zeros (sparsity) in the  $j$ -th column of  $\mathbf{S}^{*(t)}$  are given by

$$\mathbb{E}[\sum_{i=1}^m \mathbf{s}_{ij}] = \gamma m.$$

Since,  $\gamma$  can be small, we use Lemma 13(a) (McDiarmid, 1998) to derive an upper bound on the sparsity for each each column as

$$\Pr[\sum_{i=1}^m \mathbf{s}_{ij} \geq (1 + \epsilon)\gamma m] \leq \exp(-\frac{\epsilon^2 \gamma m}{2(1 + \epsilon/3)}).$$

for any  $\epsilon > 0$ . Union bounding over  $L = \min(J, K)$  independent columns of  $\mathbf{S}^{*(t)}$ .

$$\Pr\left[\bigcup_{j=1}^L \left(\sum_{i=1}^m \mathbf{s}_{ij} \leq (1 + \epsilon)\gamma m\right)\right] \geq 1 - L \exp\left(-\frac{\epsilon^2 \gamma m}{2(1 + \epsilon/3)}\right).$$

Therefore, we conclude that if  $m = \Omega(\log(L)/\gamma)$  then with probability  $(1 - \delta_s)$  the expected number of non-zeros in a column of  $\mathbf{S}^{*(t)}$  are  $\mathcal{O}(\gamma m)$ , where  $\delta_s = L \exp(-\epsilon^2 \gamma m / 2(1 + \epsilon/3))$ . ■

**Lemma 7** For any  $\epsilon > 0$  suppose we have

$$L \geq \frac{2}{(1 - (1 - \gamma)^m) \epsilon^2} \log\left(\frac{1}{\delta_p^{(t)}}\right),$$

for  $L = \min(J, K)$  and  $\gamma = \alpha\beta$ , then with probability at least  $(1 - \delta_p)$ ,

$$p = L(1 - (1 - \gamma)^m),$$

where  $\delta_p^{(t)} = \exp(-\frac{\epsilon^2}{2} L(1 - (1 - \gamma)^m))$ .

**Proof of Lemma 7** We begin by evaluating the probability that a column of  $\mathbf{S}^{*(t)}$  has a non-zero element. Let  $\mathbf{s}_{ij}$  be the indicator for the  $(i, j)$  element of  $\mathbf{S}^{*(t)}$  being non-zero, defined as

$$\mathbf{s}_{ij} = \mathbb{1}_{|\mathbf{s}_{ij}^*| > 0}.$$

Further, let  $w_j$  denote the number of non-zeros in the  $j$ -th column of  $\mathbf{S}^{*(t)}$ , defined as

$$w_j = \sum_{i=1}^m \mathbf{s}_{ij}.$$

Since each element of a column of  $\mathbf{S}^{*(t)}$  is non-zero with probability  $\gamma$ , the probability that the  $j$ -th column of  $\mathbf{S}^{*(t)}$  is an all zero vector is,

$$\Pr[w_j = 0] = (1 - \gamma)^m.$$

Therefore, the probability that the  $j$ -th column of  $\mathbf{S}^{*(t)}$  has at least one non-zero element is given by

$$\Pr[w_j > 0] = 1 - (1 - \gamma)^m. \tag{11}$$

Now, we are interested in the number of columns with at least one non-zero element among the  $L = \min(J, K)$  independent columns of  $\mathbf{S}^{*(t)}$ , which we denote by  $p$ . Specifically, we analyze the following sum

$$p = \sum_{j=1}^L \mathbb{1}_{w_j > 0}.$$

Next, using (11)  $\mathbf{E}[p] = L(1 - (1 - \gamma)^m)$ . Applying the result stated Lemma 13 (b),

$$\Pr\left[\sum_{j=1}^L \mathbb{1}_{w_j} \leq (1 - \epsilon)\mathbf{E}[p]\right] \leq \exp\left(-\frac{\epsilon^2 \mathbf{E}[p]}{2}\right) := \delta_p^{(t)}.$$

Therefore, if for any  $\epsilon > 0$  we have

$$L \geq \frac{2}{(1 - (1 - \gamma)^m) \epsilon^2} \log\left(\frac{1}{\delta_p^{(t)}}\right)$$

then with probability at least  $(1 - \delta_p)$ ,  $p = L(1 - (1 - \gamma)^m)$ , where  $\delta_p^{(t)} = \exp(-\frac{\epsilon^2}{2}L(1 - (1 - \gamma)^m))$ . ■

**Lemma 6** Suppose the input  $\widehat{\mathbf{S}}^{(t)}$  to Alg. 2 is entry-wise  $\zeta$  close to  $\mathbf{S}^{*(t)}$ , i.e.,  $|\widehat{\mathbf{S}}_{ij}^{(t)} - \mathbf{S}_{ij}^{*(t)}| \leq \zeta$  and has the correct signed-support as  $\mathbf{S}^{*(t)}$ . Then with probability atleast  $(1 - \delta_{\text{IHT}}^{(t)} - \delta_{\mathbf{B}_i}^{(t)})$ , both  $\widehat{\mathbf{B}}_i^{(t)}$  and  $\widehat{\mathbf{C}}_i^{(t)}$  have the correct support, and  $\left\| \frac{\mathbf{B}_i^{*(t)}}{\|\mathbf{B}_i^{*(t)}\|} - \pi_i \frac{\widehat{\mathbf{B}}_i^{(t)}}{\|\widehat{\mathbf{B}}_i^{(t)}\|} \right\| = \mathcal{O}(\zeta^2)$  and  $\left\| \frac{\mathbf{C}_i^{*(t)}}{\|\mathbf{C}_i^{*(t)}\|} - \pi_i \frac{\widehat{\mathbf{C}}_i^{(t)}}{\|\widehat{\mathbf{C}}_i^{(t)}\|} \right\| = \mathcal{O}(\zeta^2)$ , where  $\delta_{\text{IHT}}^{(t)} = 2m \exp(-\frac{C^2}{\mathcal{O}^*(\epsilon_i^2)}) + 2s \exp(-\frac{1}{\mathcal{O}(\epsilon_i)})$  for  $\|\mathbf{A}_i^{(t)} - \mathbf{A}_i^*\| \leq \epsilon_t$ , and  $\delta_{\mathbf{B}_i}^{(t)} = \exp(-\frac{\epsilon^2 J \alpha}{2(1+\epsilon/3)})$  for any  $\epsilon > 0$ .

**Proof of Lemma 6** The Iterative Hard Thresholding (IHT) results in an estimate of  $\mathbf{X}^{*(t)}$  which has the correct signed support [Rambhatla et al. \(2019\)](#). As a result, putting back the columns of  $\widehat{\mathbf{X}}^{(t)}$  at the respective non-zero column locations of  $\mathbf{Z}_1^{(t)\top}$ , we arrive at the estimate  $\widehat{\mathbf{S}}^{(t)}$  of  $\mathbf{S}^{*(t)}$ , which has the correct signed-support, we denote this estimate by  $\widehat{\mathbf{S}}^{(t)}$ . To recover the estimates  $\widehat{\mathbf{B}}_i^{(t)}$  and  $\widehat{\mathbf{C}}_i^{(t)}$ , we use a SVD-based procedure. Specifically, we note that,

$$\mathbf{S}_{i,:}^{*(t)\top} = \mathbf{C}_i^{*(t)} \otimes \mathbf{B}_i^{*(t)} = \text{vec}(\mathbf{B}_i^{*(t)} \mathbf{C}_i^{*(t)\top})$$

As a result, the left and right singular vectors of the rank-1 matrix  $\mathbf{B}_i^{*(t)} \mathbf{C}_i^{*(t)\top}$  are the columns  $\mathbf{B}_i^{*(t)}$  and  $\mathbf{C}_i^{*(t)}$ , respectively (up to scaling).

Let  $\mathbf{M}^{(i)}$  denote the  $J \times K$  matrix formed by reshaping the vector  $\widehat{\mathbf{S}}_{i,:}^{(t)\top}$ . We choose the appropriately scaled left and right singular vectors corresponding to the largest singular value of  $\mathbf{M}^{(i)}$  as our estimates  $\widehat{\mathbf{B}}_i^{(t)}$  and  $\widehat{\mathbf{C}}_i^{(t)}$ , respectively.

First, notice that since  $\widehat{\mathbf{S}}_{i,:}^{(t)\top}$  has the correct sign and support (due to Lemma 3), the support of matrix  $\mathbf{M}^{(i)}$  is the same as  $\mathbf{B}_i^{*(t)} \mathbf{C}_i^{*(t)\top}$ . As a result, the estimates  $\widehat{\mathbf{B}}_i^{(t)}$  and  $\widehat{\mathbf{C}}_i^{(t)}$  have the correct support, and the error is only due to the scaling ambiguity on the support. This is due to the fact that the principal singular vectors ( $\mathbf{u}$  and  $\mathbf{v}$ ) align with the sparsity structure of  $\mathbf{M}^{(i)}$  as they solve the following maximization problem also known as variational characterization of svd,

$$\sigma_1^2 = \max_{\|\mathbf{u}\|=1} \mathbf{u}^\top \mathbf{M}^{(i)} \mathbf{M}^{(i)\top} \mathbf{u} = \max_{\|\mathbf{v}\|=1} \mathbf{v}^\top \mathbf{M}^{(i)\top} \mathbf{M}^{(i)} \mathbf{v},$$

where  $\sigma_1$  denotes the principal singular value. Therefore, since  $\mathbf{M}^{(i)}$  has the correct sparsity structure as  $\mathbf{B}_i^{*(t)} \mathbf{C}_i^{*(t)\top}$  the resulting  $\mathbf{u}$  and  $\mathbf{v}$  have the correct supports as well. Here,  $\mathbf{u}$  and  $\mathbf{v}$  can be viewed as the normalized versions of  $\widehat{\mathbf{B}}_i^{(t)}$  and  $\widehat{\mathbf{C}}_i^{(t)}$ , respectively, i.e.,  $\mathbf{u} = \widehat{\mathbf{B}}_i^{(t)} / \|\widehat{\mathbf{B}}_i^{(t)}\|$  and  $\mathbf{v} = \widehat{\mathbf{C}}_i^{(t)} / \|\widehat{\mathbf{C}}_i^{(t)}\|$ .

Let  $\mathbf{E} = \mathbf{M}^{(i)} - \mathbf{B}_i^{*(t)} \mathbf{C}_i^{*(t)\top}$ , now since  $|\widehat{\mathbf{S}}_{ij}^{(t)} - \mathbf{S}_{ij}^{*(t)}| \leq \zeta$  and, from Lemma 3)  $\widehat{\mathbf{S}}_{i,:}^{(t)}$  has the correct signed-support with probability  $(1 - \delta_{\text{IHT}}^{(t)})$ , where  $\delta_{\text{IHT}}^{(t)} = 2m \exp(-\frac{C^2}{\mathcal{O}^*(\epsilon_i^2)}) + 2s \exp(-\frac{1}{\mathcal{O}(\epsilon_i)})$ , and further using Claim 1, we have that the expected number of non-zeros in  $\widehat{\mathbf{S}}_{i,:}^{(t)}$  are  $JK\alpha\beta$ , with probability atleast  $(1 - \delta_{\mathbf{B}_i}^{(t)})$ , where  $\delta_{\mathbf{B}_i}^{(t)} = \exp(-\frac{\epsilon^2 J \alpha}{2(1+\epsilon/3)})$  for some  $\epsilon > 0$ , we have

$$\|\mathbf{E}\| \leq \|\mathbf{E}\|_F \leq \sqrt{JK\alpha\beta}\zeta,$$

Then, using the result in [Yu et al. \(2014\)](#), and noting that  $\sigma_1(\mathbf{B}_i^{*(t)} \mathbf{C}_i^{*(t)\top}) = \|\mathbf{B}_i^{*(t)}\| \|\mathbf{C}_i^{*(t)}\|$  and letting

$\pi_i \in \{-1, 1\}$  (to resolve the sign ambiguity), we have that

$$\left\| \frac{\mathbf{B}_i^{*(t)}}{\|\mathbf{B}_i^{*(t)}\|} - \pi_i \mathbf{u} \right\| = \left\| \frac{\mathbf{B}_i^{*(t)}}{\|\mathbf{B}_i^{*(t)}\|} - \pi_i \frac{\widehat{\mathbf{B}}_i^{(t)}}{\|\widehat{\mathbf{B}}_i^{(t)}\|} \right\| \leq \frac{2^{3/2}(2\|\mathbf{B}_i^{(t)}\| \|\mathbf{C}_i^{(t)}\| + \sqrt{JK\alpha\beta\zeta})\sqrt{JK\alpha\beta\zeta}}{\|\mathbf{B}_i^{(t)}\|^2 \|\mathbf{C}_i^{(t)}\|^2}.$$

Next, since  $\mathbf{E}[(\mathbf{B}_{ij}^{(t)})^2 | (j, i) \in \text{supp}(\mathbf{B}^{(t)})] = 1$  as per our distributional assumptions **Def.3**, we have

$$\mathbf{E}[\|\mathbf{B}_{ji}^{*(t)}\|^2] = \mathbf{E}[(\mathbf{B}_{ji}^{*(t)})^2 | (j, i) \in \text{supp}(\mathbf{B}^{*(t)})] \Pr[(j, i) \in \text{supp}(\mathbf{B}^{*(t)})] + 0 \cdot \Pr[(j, i) \notin \text{supp}(\mathbf{B}^{*(t)})] = \alpha$$

Similarly,  $\mathbf{E}[\|\mathbf{C}_{ji}^{*(t)}\|^2] = \beta$ . Substituting,

$$\left\| \frac{\mathbf{B}_i^{*(t)}}{\|\mathbf{B}_i^{*(t)}\|} - \pi_i \frac{\widehat{\mathbf{B}}_i^{(t)}}{\|\widehat{\mathbf{B}}_i^{(t)}\|} \right\| \leq \frac{2^{3/2}(2\sqrt{JK\alpha\beta} + \sqrt{JK\alpha\beta\zeta})\sqrt{JK\alpha\beta\zeta}}{JK\alpha\beta} = \mathcal{O}(\zeta^2).$$

■

**Claim 1** Suppose  $J = \Omega(\frac{1}{\alpha})$ , then with probability at least  $(1 - \delta_{\mathbf{B}_i}^{(t)})$ ,

$$\sum_{j=1}^{JK} \text{supp}(\mathbf{S}^*(i, j)) = JK\alpha\beta,$$

where  $\delta_{\mathbf{B}_i}^{(t)} = \exp(-\frac{\epsilon^2 J \alpha}{2(1+\epsilon/3)})$  for any  $\epsilon > 0$ .

**Proof of Claim 1** In this lemma we establish an upper-bound on the number of non-zeros in a row of  $\mathbf{S}^{*(t)}$ . The  $i$ -th row of  $\mathbf{S}^{*(t)}$  can be written as  $\text{vec}(\mathbf{B}_i^{*(t)} \mathbf{C}_i^{*(t)\top})$ .

Since each element of matrix  $\mathbf{B}^{*(t)}$  and  $\mathbf{C}^{*(t)}$  are independently non-zero with probabilities  $\alpha$  and  $\beta$ , the number of non-zeros in a column  $\mathbf{B}_i^{*(t)}$  of  $\mathbf{B}^{*(t)}$  are binomially distributed. Let  $\mathbf{s}_j$  be the indicator for the  $j$ -th element of  $\mathbf{B}_i^{*(t)}$  being non-zero, defined as

$$\mathbf{s}_i = \mathbb{1}_{|\mathbf{B}^{*(t)}(j,i)| > 0}.$$

Then, the expected number of non-zeros (sparsity) in the  $i$ -th column of  $\mathbf{B}^{*(t)}$  are given by

$$\mathbf{E}[\sum \text{supp}(\mathbf{B}_i^{*(t)})] = \mathbf{E}[\sum_{j=1}^J \mathbf{s}_j] = J\alpha.$$

Since,  $\alpha$  can be small, we use Lemma 13(a) (McDiarmid, 1998) to derive an upper bound on the sparsity for each each column as

$$\Pr[\sum_{j=1}^J \mathbf{s}_j \geq (1 + \epsilon)J\alpha] \leq \exp(-\frac{\epsilon^2 J \alpha}{2(1+\epsilon/3)}) := \delta_{\mathbf{B}_i}^{(t)}. \quad (12)$$

for any  $\epsilon > 0$ .

Now we turn to the number of non-zeros in  $\mathbf{S}_i^{*(t)} = \text{vec}(\mathbf{B}_i^{*(t)} \mathbf{C}_i^{*(t)\top})$ . We first note that the  $j$ -th column of  $\mathbf{B}_i^{*(t)} \mathbf{C}_i^{*(t)\top}$  is given by  $\mathbf{C}(j, i)^{*(t)} \mathbf{B}_i^{*(t)}$ . This implies that the  $j$ -th column can be all-zeros if  $\mathbf{C}(j, i)^{*(t)} = 0$ . As a result, the expected number of non-zeros in the  $j$ -th column of  $\mathbf{B}_i^{*(t)} \mathbf{C}_i^{*(t)\top}$  can

be written as,

$$\begin{aligned}
& \mathbf{E}[\sum \text{supp}(\mathbf{C}_{ji}^{*(t)} \mathbf{B}_i^{*(t)})] \\
&= \mathbf{E}[\sum \text{supp}(\mathbf{C}_{ji}^{*(t)} \mathbf{B}_i^{*(t)}) | \mathbf{C}_{ji}^{*(t)} \neq 0] \Pr[\mathbf{C}_{ji}^{*(t)} \neq 0] + \mathbf{E}[\sum \text{supp}(\mathbf{C}_{ji}^{*(t)} \mathbf{B}_i^{*(t)}) | \mathbf{C}_{ji}^{*(t)} = 0] \Pr[\mathbf{C}_{ji}^{*(t)} = 0] \\
&= \mathbf{E}[\sum \text{supp}(\mathbf{C}_{ji}^{*(t)} \mathbf{B}_i^{*(t)}) | \mathbf{C}_{ji}^{*(t)} \neq 0] \Pr[\mathbf{C}_{ji}^{*(t)} \neq 0] = \mathbf{E}[\sum \text{supp}(\mathbf{B}_i^{*(t)})] \Pr[\mathbf{C}_{ji}^{*(t)} \neq 0].
\end{aligned}$$

Now, from (12), we have that if we choose  $J = \Omega(\frac{1}{\alpha})$  with probability atleast  $(1 - \delta_{\mathbf{B}_i}^{(t)})$ , there are  $J\alpha$  non-zeros in a column of  $\mathbf{B}^{*(t)}$ . Further since,  $\Pr[\mathbf{C}_{ji}^{*(t)} \neq 0] = \beta$ , we have that with probability atleast  $(1 - \delta_{\mathbf{B}_i}^{(t)})$ ,

$$\mathbf{E}[\sum \text{supp}(\mathbf{C}_{ji}^{*(t)} \mathbf{B}_i^{*(t)})] = J\alpha\beta.$$

Furthermore, since there are  $K$  columns in  $\mathbf{B}_i^{*(t)} \mathbf{C}_i^{*(t)\top}$ , with probability atleast  $(1 - \delta_{\mathbf{B}_i}^{(t)})$ ,

$$\mathbf{E}[\sum \text{supp}(\text{vec}(\mathbf{B}_i^{*(t)} \mathbf{C}_i^{*(t)\top}))] = \mathbf{E}[\sum_{j=1}^{JK} \text{supp}(\mathbf{S}^{*(t)}(i, j))] = JK\alpha\beta.$$

■

## D Additional Theoretical Results

**Lemma 13 Relative Chernoff McDiarmid (1998)** Let random variables  $w_1, \dots, w_\ell$  be independent, with  $0 \leq w_i \leq 1$  for each  $i$ . Let  $S_w = \sum_{i=1}^{\ell} w_i$ , let  $\nu = \mathbf{E}(S_w)$  and let  $p = \nu/\ell$ , then for any  $\epsilon > 0$ ,

- (a)  $\Pr[S_w - \nu \geq \epsilon\nu] \leq \exp(-\epsilon^2\nu/2(1 + \epsilon/3))$ ,
- (b)  $\Pr[S_w - \nu \leq -\epsilon\nu] \leq \exp(-\epsilon^2\nu/2)$ .

**Lemma 14 (From Theorem 4 in Yu et al. (2014) for singular vectors)** Given  $\mathbf{M}, \tilde{\mathbf{M}} \in \mathbb{R}^{m \times n}$ , where  $\tilde{\mathbf{M}} = \mathbf{M} + \mathbf{E}$  and the corresponding SVD of  $\mathbf{M} = \mathbf{U}\Sigma\mathbf{V}^\top$  and  $\tilde{\mathbf{M}} = \tilde{\mathbf{U}}\tilde{\Sigma}\tilde{\mathbf{V}}^\top$ , the sine of angle between the principal left (and right) singular vectors of matrices  $\mathbf{M}$  and  $\tilde{\mathbf{M}}$  is given by

$$\sin \Theta(\mathbf{U}_1, \tilde{\mathbf{U}}_1) \leq \frac{2(2\sigma_1 + \|\mathbf{E}\|_2)(\min(\|\mathbf{E}\|_2, \|\mathbf{E}\|_F))}{\sigma_1^2},$$

where  $\sigma_1$  is the principal singular value corresponding to  $\mathbf{U}_1$ . Furthermore, there exists  $\pi \in [-1, 1]$  s.t.

$$\|\mathbf{U}_1 - \pi\tilde{\mathbf{U}}_1\| \leq \frac{2^{3/2}(2\sigma_1 + \|\mathbf{E}\|_2)(\min(\|\mathbf{E}\|_2, \|\mathbf{E}\|_F))}{\sigma_1^2}.$$

**Theorem 2 (Rambhatla et al. (2019))** Suppose that assumptions A.1-A.6 hold, and Alg. 1 is provided with  $p = \tilde{\Omega}(mk^2)$  new samples generated according to model (1) at each iteration  $t$ . Then for some  $0 < \omega < 1/2$ , the estimate  $\mathbf{A}^{(t)}$  at  $(t)$ -th iteration satisfies

$$\|\mathbf{A}_i^{(t)} - \mathbf{A}_i^*\|^2 \leq (1 - \omega)^t \|\mathbf{A}_i^{(0)} - \mathbf{A}_i^*\|^2, \text{ for all } t = 1, 2, \dots$$

Furthermore, given  $R = \Omega(\log(n))$ , with probability at least  $(1 - \delta_{\text{alg}}^{(t)})$  for some small constant  $\delta_{\text{alg}}^{(t)}$ , the coefficient estimate  $\hat{\mathbf{x}}_i^{(t)}$  at  $t$ -th iteration has the correct signed-support and satisfies

$$(\hat{\mathbf{x}}_i^{(t)} - \mathbf{x}_i^*)^2 = \mathcal{O}(k(1 - \omega)^{t/2} \|\mathbf{A}_i^{(0)} - \mathbf{A}_i^*\|), \text{ for all } i \in \text{supp}(\mathbf{x}^*).$$

**Table 4:** Tensor factorization results  $\alpha, \beta = 0.005$  averaged across 3 trials. Here,  $T(\text{supp}(\widehat{\mathbf{X}}^{(T)}))$  field shows the number of iterations  $T$  to reach the target tolerance, while the categorical field,  $\text{supp}(\widehat{\mathbf{X}}^{(T)})$  indicates if the support of the recovered  $\widehat{\mathbf{X}}^{(T)}$  matches that of  $\mathbf{X}^{*(T)}$  (Y) or not (N).

$(J, K)$	Method	$m = 50$			$m = 150$			$m = 300$		
		$\frac{\ \mathbf{A}^* - \mathbf{A}^{(T)}\ _F}{\ \mathbf{A}^*\ _F}$	$\frac{\ \mathbf{X}^{*(T)} - \mathbf{X}^{(T)}\ _F}{\ \mathbf{X}^{*(T)}\ _F}$	$T(\text{supp}(\widehat{\mathbf{X}}))$	$\frac{\ \mathbf{A}^* - \mathbf{A}^{(T)}\ _F}{\ \mathbf{A}^*\ _F}$	$\frac{\ \mathbf{X}^{*(T)} - \mathbf{X}^{(T)}\ _F}{\ \mathbf{X}^{*(T)}\ _F}$	$T(\text{supp}(\widehat{\mathbf{X}}))$	$\frac{\ \mathbf{A}^* - \mathbf{A}^{(T)}\ _F}{\ \mathbf{A}^*\ _F}$	$\frac{\ \mathbf{X}^{*(T)} - \mathbf{X}^{(T)}\ _F}{\ \mathbf{X}^{*(T)}\ _F}$	$T(\text{supp}(\widehat{\mathbf{X}}))$
100	NOODL	5.38e-11	2.38e-16	245 (Y)	7.04e-11	2.24e-16	257 (Y)	5.48e-11	5.14e-13	240 (Y)
	Arora(b)	1.87e-06	1.14e-05	245 (N)	2.09e-03	1.41e-03	257 (N)	2.70e-03	2.41e-03	240 (N)
	Arora(u)	6.78e-08	1.14e-05	245 (N)	8.94e-05	7.38e-05	257 (N)	1.72e-04	8.76e-05	240 (N)
	Mairal	4.40e-03	2.00e-03	245 (N)	4.90e-03	6.87e-03	257 (N)	6.00e-03	5.10e-03	240 (N)
300	NOODL	5.72e-11	1.13e-12	61 (Y)	6.74e-11	5.44e-13	89 (Y)	9.10e-11	1.27e-12	168 (Y)
	Arora(b)	2.13e-03	2.86e-03	61 (N)	5.90e-04	4.50e-04	89 (N)	1.00e-03	1.10e-03	168 (N)
	Arora(u)	2.04e-04	2.70e-04	61 (N)	3.82e-05	4.26e-05	89 (N)	1.04e-04	1.09e-04	168 (N)
	Mairal	2.05e-01	2.28e-01	61 (N)	1.19e-02	1.09e-02	89 (N)	1.07e-02	8.40e-03	168 (N)
500	NOODL	5.49e-11	2.34e-16	50 (Y)	8.15e-11	1.25e-12	76 (Y)	9.27e-11	1.41e-12	160 (Y)
	Arora(b)	1.11e-04	1.34e-04	50 (N)	5.75e-04	5.60e-04	76 (N)	6.32e-04	2.71e-03	160 (N)
	Arora(u)	9.75e-06	1.50e-05	50 (N)	4.30e-05	4.73e-05	76 (N)	5.55e-05	2.28e-03	160 (N)
	Mairal	1.23e-01	1.10e-01	50 (N)	1.73e-02	1.20e-02	76 (N)	1.44e-02	5.99e-02	160 (N)

$(J, K)$	Method	$m = 450$			$m = 500$		
		$\frac{\ \mathbf{A}^* - \mathbf{A}^{(T)}\ _F}{\ \mathbf{A}^*\ _F}$	$\frac{\ \mathbf{X}^{*(T)} - \mathbf{X}^{(T)}\ _F}{\ \mathbf{X}^{*(T)}\ _F}$	$T(\text{supp}(\widehat{\mathbf{X}}))$	$\frac{\ \mathbf{A}^* - \mathbf{A}^{(T)}\ _F}{\ \mathbf{A}^*\ _F}$	$\frac{\ \mathbf{X}^{*(T)} - \mathbf{X}^{(T)}\ _F}{\ \mathbf{X}^{*(T)}\ _F}$	$T(\text{supp}(\widehat{\mathbf{X}}))$
100	NOODL	7.82e-11	1.79e-12	257 (Y)	8.30e-11	6.39e-13	300 (Y)
	Arora(b)	3.80e-03	3.20e-03	257 (N)	2.80e-03	3.06e-03	300 (N)
	Arora(u)	3.06e-04	1.82e-04	257 (N)	2.52e-04	2.76e-04	300 (N)
	Mairal	7.20e-03	6.90e-03	257 (N)	8.27e-03	8.07e-03	300 (N)
300	NOODL	9.43e-11	1.56e-12	201 (Y)	9.50e-11	1.63e-12	265 (Y)
	Arora(b)	9.77e-04	1.04e-03	201 (N)	1.03e-03	9.36e-04	265 (N)
	Arora(u)	1.42e-04	1.68e-04	201 (N)	1.27e-04	1.23e-04	265 (N)
	Mairal	1.47e-02	1.39e-02	201 (N)	9.40e-03	1.05e-02	265 (N)
500	NOODL	9.77e-11	1.60e-12	196 (Y)	9.72e-11	1.84e-12	264 (Y)
	Arora(b)	5.99e-04	5.30e-03	196 (N)	6.04e-04	6.37e-03	264 (N)
	Arora(u)	5.91e-05	5.30e-03	196 (N)	8.08e-05	6.37e-03	264 (N)
	Mairal	3.22e-01	2.87e-01	196 (N)	2.46e-02	1.70e-01	264 (N)

## E Experimental Evaluation

We now detail the specifics of the experiments and present additional results corresponding to section 5 for synthetic data experiments and real-world data experiments, respectively.

**Distributed Implementations:** Since the updates of  $\mathbf{X}^{(r)(t)}$  columns are independent of each other, TensorNOODL is amenable for large-scale implementation in highly distributed settings. As a result, it is especially suitable for handling the tensor decomposition applications. Furthermore, the online nature of TensorNOODL allows the algorithm to continue to learn for its lifetime.

**Note on Initialization:** For synthetic data simulations, since the ground-truth factors are known, we can initialize the dictionary factor such that the requirements of Def. 1 are met. In real-world data setting, the ground-truth is unknown and our initialization requirement can be met by existing algorithms, such as Arora et al. (2015). Consequently, in real-world experiments we use Arora et al. (2015) to initialize the dictionary factor  $\mathbf{A}^{(0)}$ . Here, we run the initialization algorithm once and communicate the estimate  $\mathbf{A}^{(0)}$  to each worker at the beginning of the distributed operation.

## E.1 Synthetic Data Simulations

### E.1.1 Experimental Set-up

**Overview of Experiments:** As discussed in section 5, we analyze the performance of the algorithm across different choices of tensor dimensions  $(J, K)$  for a fixed  $n = 300$ , its rank( $m$ ) and the sparsity of factors  $\mathbf{B}^{*(t)}$  and  $\mathbf{C}^{*(t)}$  controlled by parameters  $(\alpha, \beta)$ , for recovery of the constituent factors using three Monte-Carlo runs. For each of these runs, we analyze the recovery performance across three choices of dimensions  $J = K = \{100, 300, 500\}$ , five choices of rank  $m = \{50, 150, 300, 450, 600\}$ , and three choices of the sparsity parameters  $\alpha = \beta = \{0.005, 0.01, 0.05\}$ . The results corresponding to  $\alpha = \beta = \{0.005, 0.01, 0.05\}$  are shown in Table 4, 5, and 7, respectively.

**Data Generation:** For each experiment we draw entries of the dictionary factor matrix  $\mathbf{A}^* \in \mathbb{R}^{n \times m}$  from  $\mathcal{N}(0, 1)$ , and normalize its columns to be unit-norm. To form  $\mathbf{A}^{(0)}$  in accordance with A.2, we perturb  $\mathbf{A}^*$  with random Gaussian noise and normalized its columns, such that it is column-wise  $2/\log(n)$  away from  $\mathbf{A}^*$  in  $\ell_2$  norm sense. To form the sparse factors  $\mathbf{B}^{*(t)}$  and  $\mathbf{C}^{*(t)}$ , we assign their entries to the support independently with probability  $\alpha$  and  $\beta$ , respectively, and then draw the values on the support from the Rademacher distribution<sup>6</sup>.

**Parameters Setting:** We set TensorNOODL specific IHT parameters  $\eta_x = 0.2$  and  $\tau = 0.1$  for all experiments. As recommended by our main result, the dictionary step-size parameter  $\eta_A$  is set proportional to  $m/k$ . Since TensorNOODL, Arora(b), and Arora(u) all rely on an approximate gradient descent strategy for dictionary update, we use the same step-size  $\eta_A$  for a fair comparison depending upon the choice of rank  $m$ , and probabilities  $(\alpha, \beta)$  as per A.5; Table 6 lists the step-size choices. Here, Mairal does not employ such a parameter.

**Evaluation Metrics:** We run all algorithms till one of them achieves target tolerance (error in the factor  $\mathbf{A}$ ,  $\epsilon_T$ ) of  $10^{-10}$ , and report the number of iterations  $T$  for each experiment. Note that, in all cases TensorNOODL achieves the tolerance first, and in some cases with the algorithms considered in the analysis. Next, since recovery of  $\mathbf{A}^*$  and  $\mathbf{X}^{*(t)}$  is vital for the success of the tensor factorization task, we report the relative Frobenius error for each of these matrices, i.e., for a recovered matrix  $\widehat{\mathbf{M}}$ , we report  $\|\widehat{\mathbf{M}} - \mathbf{M}^*\|_F / \|\mathbf{M}^*\|_F$ . In addition, since the dictionary learning task focuses on recovering the sparse matrix  $\mathbf{X}^{*(t)}$ , it is agnostic to the transposed Khatri-Rao structure  $\mathbf{S}^{*(t)}$ . As a result, for recovering the sparse factors  $\mathbf{B}^{*(t)}$  and  $\mathbf{C}^{*(t)}$  is crucial for exact support recovery of  $\mathbf{X}^{*(t)}$ . Therefore, we report if the support has been exactly recovered or not.

### E.1.2 Other Considerations

**Reproducible Results:** The code employed is made available as part of the supplementary material. We fix the random seeds (to 42, 26, and 91) for each Monte Carlo run to ensure reproducibility of the results shown in this work. The experiments were run on a HP Haswell Linux Cluster. The processing of data samples for the sparse coefficients ( $\widehat{\mathbf{X}}^{*(t)}$ ) was split across 20 workers (cores), allocated a total of 200 GB RAM. For Arora(b), Arora(u), and Mairal, the coefficient recovery was switched between Fast Iterative Shrinkage-Thresholding Algorithm (FISTA) (Beck and Teboulle, 2009), an accelerated proximal gradient descent algorithm, or a stochastic-version

<sup>6</sup>The corresponding code is available at <https://github.com/srambhatla/TensorNOODL> for reproducibility.

**Table 5:** Tensor factorization results  $\alpha, \beta = 0.01$  averaged across 3 trials. Here,  $T(\text{supp}(\widehat{\mathbf{X}}^{(T)}))$  field shows the number of iterations  $T$  to reach the target tolerance, while the categorical field,  $\text{supp}(\widehat{\mathbf{X}}^{(T)})$  indicates if the support of the recovered  $\widehat{\mathbf{X}}^{(T)}$  matches that of  $\mathbf{X}^{*(T)}$  (Y) or not (N).

$(J, K)$	Method	$m = 50$			$m = 150$			$m = 300$		
		$\frac{\ \mathbf{A}^* - \mathbf{A}^{(T)}\ _F}{\ \mathbf{A}^*\ _F}$	$\frac{\ \mathbf{X}^{*(T)} - \mathbf{X}^{(T)}\ _F}{\ \mathbf{X}^{*(T)}\ _F}$	$T(\text{supp}(\widehat{\mathbf{X}}))$	$\frac{\ \mathbf{A}^* - \mathbf{A}^{(T)}\ _F}{\ \mathbf{A}^*\ _F}$	$\frac{\ \mathbf{X}^{*(T)} - \mathbf{X}^{(T)}\ _F}{\ \mathbf{X}^{*(T)}\ _F}$	$T(\text{supp}(\widehat{\mathbf{X}}))$	$\frac{\ \mathbf{A}^* - \mathbf{A}^{(T)}\ _F}{\ \mathbf{A}^*\ _F}$	$\frac{\ \mathbf{X}^{*(T)} - \mathbf{X}^{(T)}\ _F}{\ \mathbf{X}^{*(T)}\ _F}$	$T(\text{supp}(\widehat{\mathbf{X}}))$
100	NOODL	5.50e-11	5.66e-13	91 (Y)	7.59e-11	5.28e-13	112 (Y)	4.34e-11	1.62e-12	190 (Y)
	Arora(b)	3.93e-03	5.80e-03	91 (N)	2.61e-03	1.58e-03	112 (N)	2.70e-03	3.00e-03	190 (N)
	Arora(u)	4.35e-04	6.77e-04	91 (N)	6.87e-04	1.05e-04	112 (N)	2.98e-04	3.04e-04	190 (N)
	Mairal	4.03e-02	1.26e-02	91 (N)	1.34e-02	1.25e-02	112 (N)	1.18e-02	1.25e-02	190 (N)
300	NOODL	6.78e-11	5.75e-13	51 (Y)	6.35e-11	1.54e-12	76 (Y)	8.64e-11	2.06e-12	158 (Y)
	Arora(b)	4.08e-04	4.76e-04	51 (N)	1.03e-03	1.08e-03	76 (N)	1.04e-03	1.17e-02	158 (N)
	Arora(u)	1.99e-05	1.46e-05	51 (N)	1.03e-04	9.59e-05	76 (N)	2.17e-04	1.17e-02	158 (N)
	Mairal	1.64e-01	1.63e-01	51 (N)	2.61e-02	2.64e-02	76 (N)	2.81e-02	1.58e-01	158 (N)
500	NOODL	6.92e-11	8.78e-13	46 (Y)	8.77e-11	1.77e-12	77 (Y)	9.35e-11	2.12e-12	156 (Y)
	Arora(b)	3.48e-04	3.28e-04	46 (N)	5.42e-04	6.40e-03	77 (N)	5.69e-04	2.41e-03	156 (N)
	Arora(u)	2.56e-05	3.70e-05	46 (N)	4.81e-05	6.40e-03	77 (N)	1.08e-04	9.30e-03	156 (N)
	Mairal	1.56e-01	1.53e-01	46 (N)	5.28e-02	1.30e-01	77 (N)	2.53e-02	1.57e-01	156 (N)

$(J, K)$	Method	$m = 450$			$m = 500$		
		$\frac{\ \mathbf{A}^* - \mathbf{A}^{(T)}\ _F}{\ \mathbf{A}^*\ _F}$	$\frac{\ \mathbf{X}^{*(T)} - \mathbf{X}^{(T)}\ _F}{\ \mathbf{X}^{*(T)}\ _F}$	$T(\text{supp}(\widehat{\mathbf{X}}))$	$\frac{\ \mathbf{A}^* - \mathbf{A}^{(T)}\ _F}{\ \mathbf{A}^*\ _F}$	$\frac{\ \mathbf{X}^{*(T)} - \mathbf{X}^{(T)}\ _F}{\ \mathbf{X}^{*(T)}\ _F}$	$T(\text{supp}(\widehat{\mathbf{X}}))$
100	NOODL	9.48e-11	1.78e-12	211 (Y)	7.27e-11	1.94e-12	279 (Y)
	Arora(b)	3.30e-03	4.00e-03	211 (N)	3.40e-03	3.37e-03	279 (N)
	Arora(u)	8.55e-04	1.27e-03	211 (N)	6.83e-04	6.49e-04	279 (N)
	Mairal	8.00e-03	6.60e-03	211 (N)	8.77e-03	9.93e-03	279 (N)
300	NOODL	9.43e-11	2.92e-12	192 (Y)	9.33e-11	2.54e-12	252 (Y)
	Arora(b)	1.00e-03	1.25e-02	192 (N)	1.13e-03	1.54e-02	252 (N)
	Arora(u)	2.22e-04	1.25e-02	192 (N)	2.69e-04	1.54e-02	252 (N)
	Mairal	1.39e-01	2.03e-01	192 (N)	1.92e-02	1.83e-01	252 (N)
500	NOODL	9.60e-11	2.41e-12	186 (Y)	9.82e-11	2.66e-12	249 (Y)
	Arora(b)	6.49e-04	1.20e-02	186 (N)	6.55e-04	1.42e-02	249 (N)
	Arora(u)	1.39e-04	1.20e-02	186 (N)	1.55e-04	1.42e-02	249 (N)
	Mairal	6.38e-02	1.54e-01	186 (N)	1.74e-02	1.79e-01	249 (N)

of Iterative Shrinkage-Thresholding Algorithm (ISTA) (Chambolle et al., 1998; Daubechies et al., 2004) depending upon the size of the data samples available for learning (see the discussion of the coefficient update step below); see also Beck and Teboulle (2009) for details.

**Sparse Factor Recovery Considerations:** In Arora et al. (2015), the authors present two algorithms – a simple algorithm with a sample complexity of  $\bar{\Omega}(ms)$  which incurs an estimation bias (Arora(b)), and a more involved variant for unbiased estimation of the dictionary whose sample complexity was not established Arora(u). However, these algorithms do not provide guarantees on, or recover the sparse coefficients. As a result, we need to adopt an additional  $\ell_1$  minimization based coefficient recovery step. Further, the algorithm proposed by Mairal et al. (2009) can be viewed as a variant of regularized alternating least squares algorithm which employs  $\ell_1$  regularization for the recovery of the transposed Khatri-Rao structured matrix.

To form the coefficient estimates for Arora(b), Arora(u), and Mairal ‘09 we solve the Lasso (Tibshirani, 1996) program using a stochastic-version of Iterative Shrinkage-Thresholding Algorithm (ISTA) (Chambolle et al., 1998; Daubechies et al., 2004) (or Fast Iterative Shrinkage-Thresholding Algorithm (FISTA) (Beck and Teboulle, 2009) if  $p$  is small) and report the best estimate (in terms of relative Frobenius error) across 10 values of the regularization parameter. The stochastic projected gradient descent is necessary to make coefficient recovery tractable since size

**Table 6:** Choosing the step-size ( $\eta_A$ ) for the dictionary update step. We use the same dictionary update step-size parameter ( $\eta_A$ ) for TensorNOODL, Arora(b), and Arora(u) depending upon the choice of rank  $m$ , and probabilities ( $\alpha, \beta$ ), as per A.5.

Rank ( $m$ )	Step-size ( $\eta_A$ )	Notes
50	20	For $(\alpha, \beta) = 0.005$ , we use $\eta_A = 5$
150	40	–
300	40	–
450	50	–
600	50	–

of  $\mathbf{X}^{*(t)}$  grows quickly with  $(\alpha, \beta)$ . For these algorithms, coefficient estimation step the slowest step since it has to scan through different values of the regularization parameters to arrive at an estimate. In contrast, TensorNOODL does not require such an expensive tuning procedure, while providing recovery guarantees on the recovered coefficients.

Note that in practice ISTA and FISTA can be parallelized as well, but tuning of the regularization parameters still involves (an expensive) grid search. Arguably even if each step of these algorithms (ISTA and FISTA) take the same amount of time as that of TensorNOODL, the search over, say 10, values of the regularization parameters will still be take 10 times the time. As a result, TensorNOODL is an attractive choice as it does not involve an expensive tuning procedure.

**Additional Discussion:** Table 4, 5, and 7 show the results of the analysis averaged across the three Monte Carlo runs, for  $\alpha = \beta = \{0.005, 0.01, 0.05\}$ , respectively. We note that for every choice of  $(J, K)$ ,  $m$ , and  $(\alpha, \beta)$ , TensorNOODL is orders of magnitude superior to related techniques. In addition, it also recovers the support correctly in all of the cases, ensuring that the sparse factors can be recovered correctly. Specifically, the sparse factors  $\mathbf{B}^{*(t)}$  and  $\mathbf{C}^{*(t)}$  can be recovered (upto permutation and scaling) via Alg. 2.

## E.2 Real-world Data Simulations

### E.2.1 Analysis of the Enron Dataset

**Enron Email Dataset:** Sparsity-regularized ALS-based tensor factorization techniques, albeit possessing limited convergence guarantees, have been a popular choice to analyze the Enron Email Dataset ( $184 \times 184 \times 44$ ) Fu et al. (2015); Bader et al. (2006). We now use TensorNOODL to analyze the email activity of 184 Enron employees over 44 weeks (Nov. '98 –Jan. '02) during the period before and after the financial irregularities were uncovered.

The Enron Email Dataset ( $184 \times 184 \times 44$ ) consists of email exchanges between 184 employees over 44 weeks (Nov. '98 –Jan. '02) which includes the period before and after the financial irregularities were uncovered. In general, every person in an organization (like Enron) communicates with only a subset of employees, as a result the tensor of email activity (Employees vs. Employees vs. Time) naturally has the model analyzed in this work. Moreover, as pointed out by Diesner and Carley (2005) “... in 2000 Enron had a segmented culture with directives being sent from on-high and sporadic feedback”. Meaning that different units within the organization exhibited clustered communication structure. This motivates us to analyze the dataset for the presence characteristic ways of communications between different business units.

We run TensorNOODL in batch setting here, this is to showcase that in practice TensorNOODL also works in batch settings, and also to overcome the limited size of the Enron Dataset.

**Table 7:** Tensor factorization results  $\alpha, \beta = 0.05$  averaged across 3 trials. Here,  $T(\text{supp}(\widehat{\mathbf{X}}^{(T)}))$  field shows the number of iterations  $T$  to reach the target tolerance, while the categorical field,  $\text{supp}(\widehat{\mathbf{X}}^{(T)})$  indicates if the support of the recovered  $\widehat{\mathbf{X}}^{(T)}$  matches that of  $\mathbf{X}^{*(T)}$  (Y) or not (N).

$(J, K)$	Method	$m = 50$			$m = 150$			$m = 300$		
		$\frac{\ \mathbf{A}^* - \mathbf{A}^{(T)}\ _F}{\ \mathbf{A}^*\ _F}$	$\frac{\ \mathbf{X}^{*(T)} - \mathbf{X}^{(T)}\ _F}{\ \mathbf{X}^{*(T)}\ _F}$	$T(\text{supp}(\widehat{\mathbf{X}}))$	$\frac{\ \mathbf{A}^* - \mathbf{A}^{(T)}\ _F}{\ \mathbf{A}^*\ _F}$	$\frac{\ \mathbf{X}^{*(T)} - \mathbf{X}^{(T)}\ _F}{\ \mathbf{X}^{*(T)}\ _F}$	$T(\text{supp}(\widehat{\mathbf{X}}))$	$\frac{\ \mathbf{A}^* - \mathbf{A}^{(T)}\ _F}{\ \mathbf{A}^*\ _F}$	$\frac{\ \mathbf{X}^{*(T)} - \mathbf{X}^{(T)}\ _F}{\ \mathbf{X}^{*(T)}\ _F}$	$T(\text{supp}(\widehat{\mathbf{X}}))$
100	NOODL	8.03e-11	3.17e-12	46 (Y)	7.71e-11	4.92e-12	63 (Y)	9.66e-11	6.01e-12	110 (Y)
	Arora(b)	2.90e-03	3.00e-03	46 (N)	4.60e-03	3.39e-02	63 (N)	5.50e-03	4.89e-02	110 (N)
	Arora(u)	8.97e-04	8.48e-04	46 (N)	1.90e-03	3.40e-02	63 (N)	2.80e-03	4.90e-02	110 (N)
	Mairal	1.57e-01	1.67e-01	46 (N)	3.63e-02	1.54e-01	63 (N)	2.32e-02	1.99e-01	110 (N)
300	NOODL	6.51e-11	3.27e-12	42 (Y)	9.05e-11	5.61e-12	60 (Y)	9.10e-11	7.01e-12	107 (Y)
	Arora(b)	1.40e-03	1.95e-02	42 (N)	2.50e-03	3.55e-02	60 (N)	3.20e-03	5.04e-02	107 (N)
	Arora(u)	2.48e-04	1.95e-02	42 (N)	6.35e-04	3.56e-02	60 (N)	9.48e-04	5.05e-02	107 (N)
	Mairal	6.24e-02	1.11e-01	42 (N)	3.05e-02	1.59e-01	60(N)	1.91e-02	2.09e-01	107 (N)
500	NOODL	7.72e-11	3.86e-12	42 (Y)	8.44e-11	5.63e-12	59 (Y)	9.64e-11	7.34e-12	106 (Y)
	Arora(b)	1.30e-03	2.02e-02	42 (N)	2.10e-03	3.55e-02	59 (N)	2.80e-03	5.03e-02	106 (N)
	Arora(u)	1.39e-04	2.02e-02	42 (N)	3.82e-04	3.56e-02	59 (N)	5.66e-04	5.05e-02	106 (N)
	Mairal	6.12e-02	1.10e-01	42 (N)	2.93e-02	1.58e-01	59 (N)	1.80e-02	2.11e-01	106 (N)

$(J, K)$	Method	$m = 450$			$m = 500$		
		$\frac{\ \mathbf{A}^* - \mathbf{A}^{(T)}\ _F}{\ \mathbf{A}^*\ _F}$	$\frac{\ \mathbf{X}^{*(T)} - \mathbf{X}^{(T)}\ _F}{\ \mathbf{X}^{*(T)}\ _F}$	$T(\text{supp}(\widehat{\mathbf{X}}))$	$\frac{\ \mathbf{A}^* - \mathbf{A}^{(T)}\ _F}{\ \mathbf{A}^*\ _F}$	$\frac{\ \mathbf{X}^{*(T)} - \mathbf{X}^{(T)}\ _F}{\ \mathbf{X}^{*(T)}\ _F}$	$T(\text{supp}(\widehat{\mathbf{X}}))$
100	NOODL	8.92e-11	7.29e-12	115 (Y)	8.71e-11	1.06e-11	131 (Y)
	Arora(b)	7.50e-03	6.17e-02	115 (N)	9.16e-03	7.36e-02	131 (N)
	Arora(u)	4.40e-03	6.19e-02	115 (N)	5.70e-03	7.40e-02	131 (N)
	Mairal	8.79e-02	2.27e-01	115 (N)	2.81e-02	2.56e-01	131 (N)
300	NOODL	9.20e-11	8.41e-12	110 (Y)	8.49e-11	9.03e-12	128 (Y)
	Arora(b)	4.00e-03	6.16e-02	110 (N)	4.90e-03	7.39e-02	128 (N)
	Arora(u)	1.40e-03	6.18e-02	110 (N)	1.83e-03	7.42e-02	128 (N)
	Mairal	4.85e-02	2.19e-01	110 (N)	2.32e-02	2.63e-01	128 (N)
500	NOODL	8.95e-11	8.21e-12	109 (Y)	9.06e-11	9.29e-12	127 (Y)
	Arora(b)	3.60e-03	6.21e-02	109 (N)	4.40e-03	7.40e-02	127 (N)
	Arora(u)	8.54e-04	6.23e-02	109 (N)	1.10e-03	7.44e-02	127 (N)
	Mairal	4.62e-02	2.20e-01	109 (N)	4.05e-02	2.56e-01	127 (N)

**Data Preparation and Parameters:** For TensorNOODL and Mairal ‘09, we use the initialization algorithm of Arora et al. (2015), which yielded 4 dictionary elements. Following this, we use these techniques in batch setting to simultaneously identify email activity patterns and cluster employees. We also compare our results to Fu et al. (2015), which just aims to cluster the employees by imposing sparsity constraint on one of the factors, and does not learn the patterns. As opposed to Fu et al. (2015), TensorNOODL did not require us to guess the number of dictionary elements to be used. We use Alg. 2 to identify the employees corresponding to email activity patterns from the recovered sparse factors. As in case of Fu et al. (2015), we transform each non-zero element  $\underline{\mathbf{Z}}(i, j, k)^{(t)}$  of the dataset as follows to compress its dynamic range,

$$\underline{\mathbf{Z}}(i, j, k)^{(t)} = \log_2(\underline{\mathbf{Z}}(i, j, k)) + 1.$$

We also scale all elements by the largest element magnitude and subtract the mean (over the temporal aspect) from the non-zero fibers. We initialize the dictionary using the algorithm presented in Arora et al. (2015) for TensorNOODL and Mairal ‘09, resulting in 4 dictionary elements. As with synthetic data experiments, we set  $\eta_x = 0.2$ ,  $\tau = 0.1$  and  $C = 1$ . We set the dictionary update step-size  $\eta_A = 10$ , and run TensorNOODL in batch setting for 100 iterations. We recover the sparse factors  $\mathbf{B}^{*(t)}$  and  $\mathbf{C}^{*(t)}$  using our untangling Alg. 2. To compile the results, we ignore the entries with magnitude smaller than 5% of the largest entry in that sparse factor column.

**Evaluation Specifics:** As in Fu et al. (2015), we use cluster purity (False Positives/Cluster Size) as the measure of the clustering performance. To this end, we also compare our results with Fu et al. (2015). Note that Fu et al. (2015) solves a regularized least squares-based formulation for low-rank non-negative tensor factorization, wherein one of factor is sparse (corresponds to employees) and the others have controlled Frobenius norms. Here, the non-zero entries of the sparse factor gives insights into the employees who exhibit similar behaviour. Unlike TensorNOODL and Mairal ‘09, this procedure however does not recover the email patterns of interest.

**Discussion:** The results of the decomposition are shown in Fig. 6. The Enron organizational structure has four main units, namely, ‘Legal’, ‘Traders’, ‘Executives’, and ‘Pipeline’, which coincides with the number of dictionary elements recovered by TensorNOODL. Specifically, as opposed to Fu et al. (2015), which take the number of clusters to be found as an input, TensorNOODL leverages the model selection performed by initialization algorithms. Furthermore, along with recovering the email activity patterns, TensorNOODL is also superior in terms of the clustering purity as compared to other techniques as inferred from the False Positives to Cluster-size ratio (Fig. 6). The email activity patterns show how different group activities changed as time unfolded. In line with Diesner and Carley (2005), we observe that during the crisis the employees of different divisions indeed exhibited cliquish behavior. These results illustrate that our model (and algorithm) can be used to study organizational behavior via their communication activity. Note that here we use TensorNOODL in the batch setting, i.e., we reuse samples. This shows that empirically our algorithm can be used in the batch setting also, although our analysis applies to the online setting. We leave the analysis of the batch setting to future work.

### E.2.2 Analysis of the NBA Dataset

The online nature of TensorNOODL makes it suitable for learning tasks where data arrives in a streaming fashion. In this application, we analyze the National Basketball Association (NBA) weekly shot patterns of high scoring players against different teams. In this online mining application, our aim is to tease apart the relationships between shot selection of different players against different teams. Here, our model enables us to cluster the players and the teams, in addition to recovering the shot patterns shared by them.

We form the NBA shot pattern dataset by collecting weekly shot patterns of players for each week (27 weeks) of the 2018 – 19 regular season of the NBA league. Each of these tensors consists of the locations of all shots attempted by players (above 80<sup>th</sup> percentile of the 497 active players, which gives us 100 high-scorers) against (30) opponent teams in a week of the 2018 – 19 regular season of the NBA league. To form the tensor we divide the half court into  $10 \times 12$  blocks, and sum all the shots from a block to compile the shot pattern. We then vectorize this 2-D shot pattern, which constitutes a fiber of the tensor. Since players don’t play every other team in a week, the resulting weekly shot pattern tensor  $\underline{\mathbf{Z}}^{(t)} \in \mathbb{R}^{100 \times 30 \times 120}$  has only a few non-zero fibers, and fits the model of interest shown in Fig. 1. In case a player plays against a team more than once a week, we average the shot patterns to form the weekly shot pattern tensor.

**Data Preparation and Parameters:** To prepare the data, we element-wise transform each non-zero element of the weekly shot pattern tensor ( $\underline{\mathbf{Z}}^{(t)}(i, j, k)$ ) as  $\underline{\mathbf{Z}}^{(t)}(i, j, k) = \log_2(\underline{\mathbf{Z}}^{(t)}(i, j, k)) + 1$  to reduce its dynamic range. We then subtract the mean along the shot pattern axis to reduce the effect of any dominant shot locations. We form the initial estimate of the incoherent dictionary

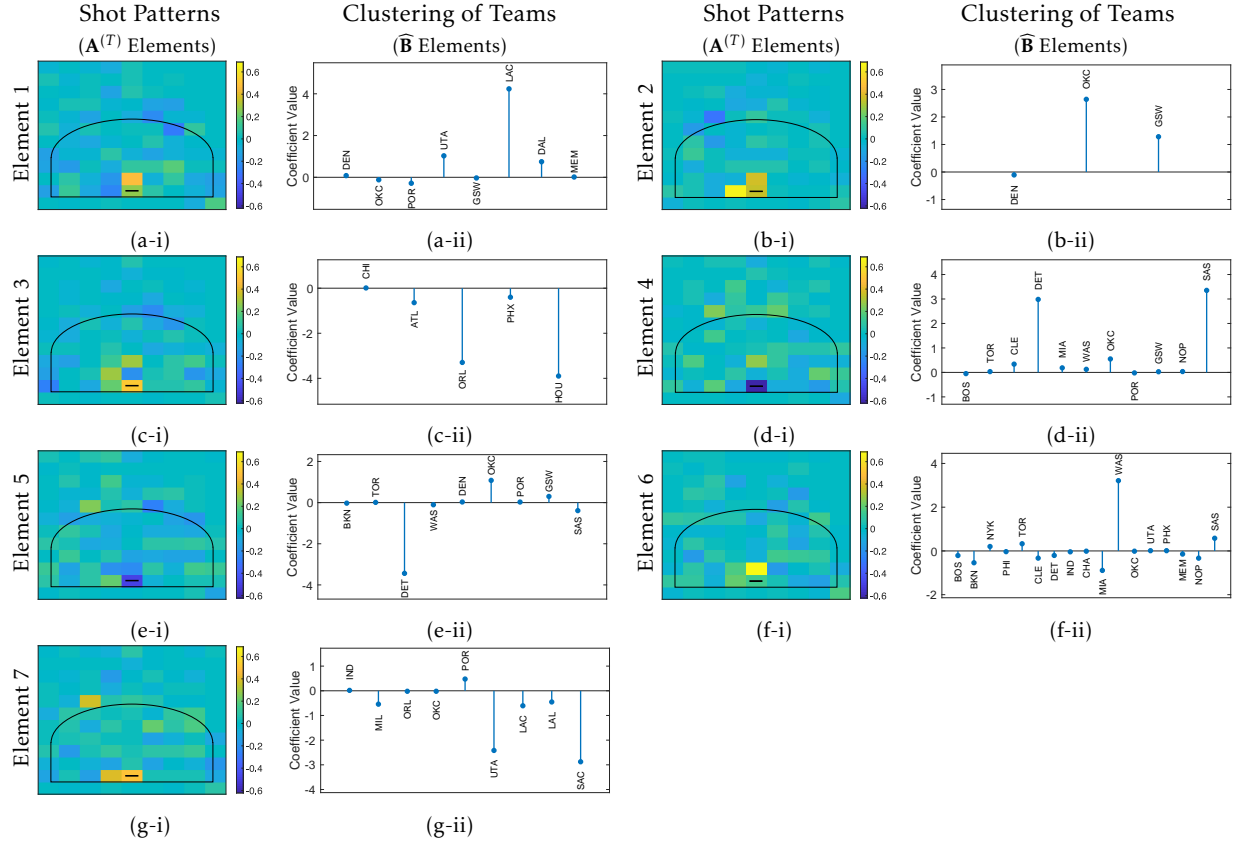


**Figure 8:** Shot Patterns and Teams in the NBA dataset. Panels (a-g)-i show dictionary factor ( $\mathbf{A}^{(T)}$ ) columns (elements) reshaped into a matrix to show different recovered shot patterns. Here, the 3-point line and the rim is indicated in black. Corresponding sparse factor ( $\widehat{\mathbf{B}}$ ) representing Teams are shown in panels (a-g)-ii.

factor ( $\mathbf{A}^*$ ) from the 2017 – 18 regular season data of the top 80<sup>th</sup> percentile players using the initialization algorithm presented in [Arora et al. \(2015\)](#). We use  $\eta_x = 0.1$ ,  $\tau = 0.2$ ,  $C = 1$  and  $\eta_A = 10$  as the TensorNOODL parameters to analyze the data.

**Evaluation Specifics:** We focus on the games in the week 10 of the 2018 – 19 regular season to illustrate the application of TensorNOODL for this sports analytics task. Our analysis yields the shared shot selection structure of different players and teams.

**Discussion:** In the main paper, we analyze the similarity between two players – James Harden and Devin Booker – who incidentally at that time were seen as having similar styles [Rafferty \(2018\)](#); [Uggetti \(2018\)](#). In this case, our results corroborate that the shot selection patterns of these two players is indeed similar. This is indicated by sparse factor corresponding to the players. In Fig. 8, and Table. 8 we show the recovered dictionary elements ( $\mathbf{A}^{(T)}$ ) or the shot patterns and the corresponding clustering of teams ( $\widehat{\mathbf{B}}^{(T)}$ ), and the players ( $\widehat{\mathbf{C}}^{(T)}$ ), respectively, for week 10. For both  $\widehat{\mathbf{B}}^{(T)}$  and  $\widehat{\mathbf{C}}^{(T)}$  we show the elements whose corresponding magnitude is greater than  $10^{-2}$ . These preliminary results motivate further exploration of TensorNOODL for sports analytics applications. The theoretical guarantees coupled with its amenability in highly distributed online processing, makes TensorNOODL especially suitable for such application, where we can learn and make decisions on-the-fly.

**Table 8: Analysis of Sparse factor corresponding to Players ( $\hat{C}$ )**

Players corresponding to element 1			Players corresponding to element 2		
Players	Position	Coefficient Value	Players	Position	Coefficient Value
Harrison Barnes	Small forward / Power forward	-0.2770	Harrison Barnes	Small forward / Power forward	-0.0187
Stephen Curry	Point guard	-0.7620	Danilo Gallinari	Power forward / Small forward	-0.0515
Kevin Durant	Small forward	-0.0707	Tobias Harris	Small forward / Power forward	-0.2729
Nikola Jokic	Center	0.5040	Donovan Mitchell	Shooting guard	0.6536
CJ McCollum	Shooting guard	-0.0771	Karl-Anthony Towns	Center	0.5449
Donovan Mitchell	Shooting guard	0.0414	Andrew Wiggins	Shooting guard / Small forward	0.4454
Jamal Murray	Point guard / Shooting guard	-0.1677	Players corresponding to element 3		
Jusuf Nurkic	Center	0.0352	Players	Position	Coefficient Value
Ricky Rubio	Point guard	0.0191	LaMarcus Aldridge	Power forward / Center	-0.2248
Klay Thompson	Shooting guard	-0.2128	Trevor Ariza	Small forward / Shooting guard	0.3195
Russell Westbrook	Point guard	-0.0208	DeMar DeRozan	Small forward / Shooting guard	-0.6716
Lou Williams	Shooting guard / Point guard	-0.0198	Bryn Forbes	Shooting guard / Point guard	0.1241
Players corresponding to element 4			Justin Holiday	Shooting guard / Small forward	0.1074
Players	Position	Coefficient Value	Josh Richardson	Shooting guard / Small forward	0.6049
Bojan Bogdanovic	Small forward	-0.0275	Justise Winslow	Point guard	-0.0580
Devin Booker	Shooting guard / Point guard	0.0114	Players corresponding to element 5		
Clint Capela	Center	-0.2256	Players	Position	Coefficient Value
Willie Cauley-Stein	Center / Power forward	-0.0150	Devin Booker	Shooting guard / Point guard	0.0104
Evan Fournier	Shooting guard / Small forward	0.2032	Clint Capela	Center	0.0210
James Harden	Shooting guard / Point guard	0.1992	Luka Doncic	Guard / Small forward	-0.0162
Buddy Hield	Shooting guard	-0.0198	Eric Gordon	Shooting guard / Small forward	0.0150
Jeremy Lamb	Shooting guard / Small forward	-0.1468	James Harden	Shooting guard / Point guard	0.0678
Derrick Rose	Point guard	0.4961	Tobias Harris	Small forward / Power forward	-0.0247
Ricky Rubio	Point guard	0.0198	Joe Ingles	Small forward	0.1005
Pascal Siakam	Power forward	-0.0244	Josh Jackson	Small forward / Shooting guard	-0.0100
Karl-Anthony Towns	Center	0.7711	Donovan Mitchell	Shooting guard	0.0984
Kemba Walker	Point guard	0.0331	Kelly Oubre Jr.	Small forward / Shooting guard	-0.0143
Andrew Wiggins	Shooting guard / Small forward	-0.0119	Derrick Rose	Point guard	0.6507
Thaddeus Young	Power forward	-0.0148	Ricky Rubio	Point guard	0.0488
Trae Young	Point guard	0.0415	Karl-Anthony Towns	Center	0.6924
Players corresponding to element 6			Kemba Walker	Point guard	0.1670
Players	Position	Coefficient Value	Andrew Wiggins	Shooting guard / Small forward	0.2000
Deandre Ayton	Center / Power forward	0.0640	Lou Williams	Shooting guard / Point guard	0.0196
Eric Bledsoe	Point guard	0.0527	Players corresponding to element 6 continued...		
Bojan Bogdanovic	Small forward	-0.1353	Players	Position	Coefficient Value
Devin Booker	Shooting guard / Point guard	0.4668	Jeremy Lamb	Shooting guard / Small forward	-0.0229
Jimmy Butler	Shooting guard / Small forward	-0.0157	Kawhi Leonard	Small forward	-0.0384
Kentavious Caldwell-Pope	Shooting guard	0.0507	Brook Lopez	Center	0.0194
Clint Capela	Center	0.6348	Lauri Markkanen	Power forward / Center	0.0186
Willie Cauley-Stein	Center / Power forward	-0.0303	CJ McCollum	Shooting guard	0.0148
Jordan Clarkson	Point guard / Shooting guard	-0.0141	Khris Middleton	Shooting guard / Small forward	0.0617
John Collins	Power forward	0.0948	Jusuf Nurkic	Center	0.0121
DeAaron Fox	Point guard	0.0148	Cedi Osman	Small forward / Shooting guard	-0.0260
Aaron Gordon	Power forward / Small forward	0.0978	Kelly Oubre Jr.	Small forward / Shooting guard	-0.1673
Eric Gordon	Shooting guard / Small forward	0.1861	JJ Redick	Shooting guard	-0.0474
James Harden	Shooting guard / Point guard	0.2834	Terrence Ross	Small forward / Shooting guard	0.0216
Buddy Hield	Shooting guard	-0.0135	Pascal Siakam	Power forward	-0.0512
Justin Holiday	Shooting guard / Small forward	0.0756	Ben Simmons	Point guard / Forward	-0.0166
Josh Jackson	Small forward / Shooting guard	0.0339	Myles Turner	Center	-0.3469
LeBron James	Small forward / Power forward	-0.1362	Nikola Vucevic	Center	0.0827
Kyle Kuzma	Power forward	-0.0272	Thaddeus Young	Power forward	-0.0494
Players corresponding to element 7			Trae Young	Point guard	-0.1377
Players	Position	Coefficient Value	Players corresponding to element 7 continued...		
Harrison Barnes	Small forward / Power forward	0.0330	Players	Position	Coefficient Value
Mike Conley	Point guard	0.2633	Jerami Grant	Forward	-0.0767
Jae Crowder	Small forward	0.0454	Joe Harris	Shooting guard / Small forward	-0.0120
Stephen Curry	Point guard	0.0429	Jrue Holiday	Point guard / Shooting guard	-0.2258
Anthony Davis	Power forward / Center	-0.3173	Kyrie Irving	Point guard	-0.0128
Luka Doncic	Guard / Small forward	-0.0239	Julius Randle	Power forward / Center	-0.0266
Kevin Durant	Small forward	-0.5214	DAngelo Russell	Point guard	-0.0365
Marc Gasol	Center	0.0655	Dennis Schroder	Point guard / Shooting guard	0.1013
Paul George	Small forward	-0.6895	Klay Thompson	Shooting guard	0.0322
			Dwyane Wade	Shooting guard	0.0208
			Justise Winslow	Point guard	0.0431